Supplementary information for "Modeling of coseismic and transient deformation associated with the 1995 Colima-Jalisco and 2003 Tecomán thrust earthquakes: Mexico subduction zone"

by Cosenza-Muralles *et al.*

The supplementary materials in this document include:

- A summary of the results from the inversion of the GPS position time series without corrections for the viscoelastic effects from the 1995 Colima-Jalisco and the 2003 Tecomán earthquakes (Section S1).
- Supplementary Tables S1 to S12, which are referenced in the main document (Section S2).
- Supplementary Figures S1 to S21, which are referenced in the main document (Section S3).
- A description of the separate files provided with this document (Section S4).

The additional files include:

- The coseismic slip and afterslip solutions from our preferred model (.nod and .atr files):
  - 1995EQ_coseismic_slip.nod
  - 1995EQ_afterslip.nod
  - 2003EQ_coseismic_slip.nod
  - 2003EQ_afterslip.nod
  - 1995EQ_coseismic_slip.atr
  - 1995EQ_afterslip.atr
  - 2003EQ_coseismic_slip.atr
  - 2003EQ_afterslip.atr
- The interseismic site velocities resulting from the models with different Maxwell times for the viscoelastic corrections, and those from the model with no correction are also provided in separate .txt files:
  - vels_tm_2.5years.txt
  - vels_tm_4years.txt
  - vels_tm_8years.txt
  - vels_tm_15years.txt
  - vels_tm_25years.txt
  - vels_tm_40years.txt
  - vels_no_corr.txt

S1 MODEL WITH NO VISCOELASTIC GPS TIME SERIES CORRECTIONS

As is described in the main document, we used TDEFNODE to invert our GPS position time series absent any corrections for the viscoelastic effects of the 1995 and 2003 earthquakes to create a baseline reference model and its associated fits for comparison to the six models that we derived with viscoelastic corrections. Similar to those six TDEFNODE models, the parameters estimated for this afterslip-only model include the 1995 and 2003 coseismic and afterslip solutions, logarithmic decay constants for the afterslip after each earthquake, and an interseismic velocity at each GPS site represented in the input data. Overall, the TDEFNODE output consisted of 1166 estimated parameters constrained by 201,510 observations, consisting of the north, east and vertical daily position estimates at 62 GPS sites (excluding all vertical observations at continuous stations INEG, CUVA, UAGU, and TNZA, where the vertical rates appear to be biased by rapid subsidence attributable to groundwater withdrawal). Misfit F (main document Eq. 3) for this best-fitting model is 14.7. The wrms misfits for the model are 1.9-4.9 mm in the horizontal position components at continuous sites and 5.4-5.8 mm at the campaign sites. The wrms misfits to the noisier vertical daily positions are 7.4 mm at the continuous sites and 15.3 mm at the campaign sites.

The best-fitting coseismic slip solution for the 1995 Colima-Jalisco earthquake (Figs S7h and S19a) agrees well with previous seismic estimates (*e.g.* Courboulex *et al.* 1997; Escobedo *et al.* 1998; Mendoza and Hartzell 1999) and with the GPS-derived solution from Hutton *et al.* (2001). Most of the seismic energy (~66%) was released at depths of 5 to 20 km, consistent with seismic constraints and deeper than our estimate using shorter time series (main document Section 5.1). The region of primary rupture coincides closely with the region of aftershocks determined by Pacheco *et al.* (1997). The geodetic coseismic moment we estimate is 9.8×10^{20} N·m, corresponding to $M_w = 7.9$ for a standard value of 40 GPa for the shear modulus.

The cumulative estimated moment released by the afterslip triggered by the 1995 Colima-Jalisco earthquake was 13.2×10^{20} N·m ($M_w = 8.0$), equivalent to ~130 percent of the coseismic moment release (Table S5). Eighty seven percent of that moment occurred at depths below 15 km, downdip from the coseismic rupture zone (Fig. S19 and Table S9). This result agrees with respect to five of the six Maxwell times we explored in our analysis: our inversions of the 1993-2020 data corrected for viscoelastic deformation modeled with Maxwell times equal to or longer than 4 yr all indicate that 80 percent or more of the afterslip occurred below 15 km (Table S9). Absent any correction for likely viscoelastic deformation, the estimated logarithmic decay constant for afterslip is 82 ± 1 days, 6-16 times longer than the 5-14 day decay times estimated for the six models we derived with viscoelastic rebound corrections (Table S5). The much longer decay constant is required because viscoelastic deformation that decays over time scales of years to decades is not corrected for in this afterslip-only model.

The coseismic slip estimated for the 2003 earthquake was largely confined to the Manzanillo Trough (Figs S8 and S20a), with 91% of the seismic energy released between depths of 10 and 40 km (Table S3). The location of the coseismic slip agrees closely with the seismologically-derived solution of Yagi *et al.* (2004) (shown by the red lines in Fig. S20a) and also with the seismologic slip solution of Quintanar *et al.* (2010) and the GPS-derived solution of Schmitt *et al.* (2007), as well as with our solutions with viscoelastic corrections (Fig. S8). The estimated coseismic moment of 2.49×10^{20} N·m ($M_w = 7.5$) is ~25 percent larger than the estimates derived when applying viscoelastic corrections to the data (Table S3).

For the afterslip triggered by the 2003 earthquake, the estimated cumulative moment was of 3.0×10^{20} N·m ($M_w = 7.6$), equivalent to 120 percent of the coseismic moment release (Table S7). Eighty-nine percent of the afterslip energy was released at depths of 15-60 km (Fig. S20b and Table S9), *i.e.* at the same depths as, or downdip from, the 2003 earthquake rupture zone and mostly confined along strike by the lateral boundaries of the coseismic rupture. The energy released by afterslip at depths shallower than 15 km amounts only to 11 percent of the total (Table S9). The decay constant estimated for the afterslip triggered by the 2003 earthquake is 64 ± 1 days, much longer than 3-15 day estimates for TDEFNODE models derived from the GPS data with viscoelastic rebound corrections (Table S7). As is true for the 1995 afterslip decay constant that was estimated without any viscoelastic correction to the underlying GPS data (see above), the 64-day estimated decay constant is much longer because viscoelastic deformation that decays over time scales of years to decades is ignored in this afterslip-only model.

REFERENCES

Courboulex, F., Singh, S.K., & Pacheco, J.F., 1997. The 1995 Colima-Jalisco, Mexico, earthquake (M_w 8): A study of the rupture process, *Geophys. Res. Lett.,* **24**(9), 1019-1022.

Escobedo, D., Pacheco, J.F. & Suárez, G., 1998. Teleseismic body-wave analysis of the 9 October, 1995 (Mw = 8.0), Colima-Jalisco earthquake, and its largest foreshock and aftershock, *Geophys Res Lett*, **25**(4), 547-550.

Hutton, W., DeMets, C., Sánchez, O., Suárez, G. & Stock, J., 2001. Slip kinematics and dynamics during and after the 1995 October 9 Mw=8.0 Colima-Jalisco earthquake, Mexico, from GPS geodetic constraints, *Geophys. J. Inter*., **146**, 637–658.

Mendoza, C. & Hartzell, S., 1999. Fault-slip distribution of the 1995 Colima-Jalisco, Mexico, earthquake, *Bull. Seismol. Soc. Am*., **89**(5), 1338-1344.

Pacheco, J., Singh, S.K., Domínguez, J., Hurtado, A., Quintanar, L., Jiménez, Z., Yamamoto, J., Gutiérrez, C., Santoyo, M., Bandy, W., Guzmán, M. & Kostoglodov, V., 1997. The October 9, 1995 Colima-Jalisco, Mexico earthquake (M_w 8): An aftershock study and a comparison of the earthquake with those of 1932, *Geophys. Res. Lett.*, **24**(17), 2223-2226.

Quintanar, L., Rodríguez-Lozoya, H.E., Ortega, R., Gómez-González, J.M., Domínguez, T., Javier, C., Alcántara, L. & Rebollar, C.J., 2010. Source characteristics of the 22 January 2003 M_w = 7.5 Tecoman, Mexico, Earthquake: New insights, *Pure Appl. Geophys*., **168**, 1339–1353, DOI 10.1007/s00024-010-0202-1.

Schmitt, S.V., DeMets, C., Stock, J., Sánchez, O., Márquez-Azúa, B. & Reyes, G., 2007. A geodetic study of the 2003 January 22 Tecoman, Colima, Mexico earthquake, *Geophys. J. Int.,* **169**, 389–406, doi: 10.1111j.1365-246X.2006.03322.x.

Yagi, Y., Mikumo, T., Pacheco, J. & Reyes, G., 2004. Source rupture process of the Tecoman, Colima, Mexico Earthquake of 22 January 2003, determined by joint inversion of teleseismic body-wave and near-source data, *Bull. Seismol. Soc. Am.,* **94**(5), 1795-1807.

S2 SUPPLEMENTARY TABLES

Table S1: GPS site information

Site ID	Latitude* °N	Longitude* °E	Elevation† m	Time span	Observation days
ANIG	21.0538	-104.5207	1000.18	2006.8411 - 2018.3260	1880
AUTA	19.7482	-104.3293	870.83	1996.1803 - 2009.1863	26
AVAL	19.4808	-103.6841	1618.24	1995.1890 - 2004.1585	24
AYUT	20.1885	-104.3745	1650.03	1995.1671 - 2009.1863	28
CALC	18.0790	-102.7619	32.22	2007.9397 - 2013.6548	1111
CEBO	20.0896	-103.1608	2004.38	1995.1890 - 2007.1918	21
CGUZ	19.7300	-103.4461	1736.02	1996.1612 - 2007.1890	20
CHAC	20.3835	-105.4289	272.10	1995.1781 - 2009.1781	38
CHAM	19.5271	-105.0842	-11.90	1995.1671 - 2009.1890	39
CHMC	19.4980	-105.0448	82.85	2006.8329 - 2014.8027	1893
COJB	19.5155	-103.5699	2326.52	2011.6192 - 2015.0712	1007
COLI	19.2491	-103.7182	512.93	1993.2822 - 2019.5945	6604
COLW	19.5154	-103.6399	2814.90	2011.3315 - 2014.0822	951
COOB	19.3814	-103.6744	1212.48	1997.4685 - 2014.0712	2583
COPE	19.5269	-103.6109	3161.53	2011.3288 - 2014.0000	968
COPN	19.5289	-103.6240	3042.24	2011.3342 - 2013.9973	966
COS2	20.2930	-103.3246	1727.72	1996.1694 - 2007.1945	20
CRIP	19.0313	-104.3328	-5.75	1995.1671 - 2003.4438	327
CUVA	20.5356	-103.9669	1222.78	2009.1945 - 2018.1507	3154
FARO	18.3446	-103.5087	35.73	2006.7233 - 2010.3342	1281
GUAC	20.5006	-104.3540	1575.01	1995.1671 - 2009.1781	28
GUFI	19.5062	-104.5495	265.50	1996.1667 - 2009.1945	46
IITJ	20.6845	-103.4460	1656.99	2003.9562 - 2007.3342	1061
INEG	21.8562	-102.2842	1889.09	1995.1233 - 2019.5945	7321
LIM2	20.3346	-103.5282	1653.29	1998.1260 - 2007.1918	17
LIMA	20.3700	-103.5476	2106.51	1996.1913 - 1998.0849	5
LZCR	17.9394	-102.1783	-8.50	2008.9290 - 2014.4329	1010
MANZ	19.0639	-104.2981	-14.18	1999.2986 - 2006.4000	1165
MASC	20.5347	-104.7967	1221.62	2009.1726 - 2018.1507	3064
MCAB	21.0916	-103.4935	1680.06	1995.1671 - 2004.1667	17
MELA	19.2202	-104.7179	57.46	1996.1612 - 2009.1945	36
MILN	19.7369	-105.2194	9.71	2000.1503 - 2009.1890	29
MIRA	18.9227	-104.0210	-0.61	2001.5479 - 2007.1781	32
MMIG	18.2885	-103.3455	41.44	2006.8274 - 2016.2760	1829
MNZO	19.0639	-104.2982	-13.88	2011.8411 - 2014.1151	659
MPR1	20.6790	-105.2492	10.94	2008.3142 - 2019.5945	3922
NOVI	18.8722	-103.6764	95.19	2001.5534 - 2007.1699	25
NVDO	19.5656	-103.6165	4004.38	2004.8005 - 2014.4247	2237
PENA	19.3905	-104.1014	1489.98	2007.0849 - 2018.7260	3753
PORT	20.0145	-105.4699	9.00	2000.1421 - 2004.1393	13
PURI	19.6651	-104.6371	376.41	1995.1890 - 2013.2137	2215
PZUL	20.0640	-105.5076	183.79	2007.2000 - 2014.6877	1565
SEBA	20.6989	-104.8710	1971.67	1995.1781 - 2009.1753	25
SJDL	18.5765	-103.6629	24.94	1995.1671 - 2007.1699	43
TAPA	19.8311	-103.7971	1961.73	1995.1890 - 2007.1918	25
TECO	18.9845	-103.8610	213.53	2007.1397 - 2018.8329	3100

Continued on next page

Table S1 – continued from previous page

Site ID	Latitude* °N	Longitude* °E	Elevation† m	Time span	Observation days
TENA	19.2829	-104.8750	-5.82	2000.1503 - 2005.1315	23
TNCC	18.7911	-103.1730	1074.24	2015.8027 - 2018.8329	912
TNCM	19.4981	-105.0448	83.09	2014.6877 - 2018.8329	1207
TNCT	19.6811	-105.2588	-8.68	2017.0384 - 2018.5479	508
TNLC	19.5061	-104.5492	267.85	2015.8137 - 2018.8329	907
TNMR	18.2885	-103.3455	41.30	2014.6904 - 2018.7479	660
TNMZ	19.1236	-104.4015	-5.81	2015.4767 - 2018.2466	651
TNTM	19.2391	-104.7899	12.74	2017.0466 - 2018.8329	616
TNZA	19.9989	-102.2903	1556.78	2015.4575 - 2017.4849	57
TOMA	19.9603	-105.2693	20.46	1996.1639 - 1997.0877	3
UAGU	21.9185	-102.3150	1860.63	2010.0000 - 2018.8329	1995
UCOL	19.1241	-104.4015	-9.71	2002.1425 - 2015.4740	3407
UGEO	20.6939	-103.3500	1533.79	2000.1612 - 2019.5945	3303
UMON	20.7373	-103.4532	1622.48	1996.1913 - 1999.4575	13
VICT	18.7675	-103.3961	880.32	1995.1781 - 2007.1726	36
VALL	20.6579	-105.2429	-17.83	2013.8493 - 2014.8384	354

*Site coordinates are in IGS14/ITRF2014 for the first day of measurements at each site.
†Site elevations are specified relative to the WGS84 reference ellipsoid for the first day of measurements at each site.

Table S2: Coseismic displacements from the 1995 Colima-Jalisco earthquake at GPS sites active during the earthquake.

Site	North (mm) ±1 mm	East (mm) ±1 mm	Vertical (mm) ±2 mm
AVAL	-74	-106	-13
AYUT	-162	-103	-4
CEBO	-42	-50	1
CHAC	-88	-10	-17
CHAM	-837	-463	-207
COLI	-55	-101	-12
CRIP	-386	-283	-37
GUAC	-112	-62	2
INEG	-15	-13	3
MCAB	-41	-29	4
PURI	-407	-263	-74
SEBA	-94	-30	-2
SJDL	-16	-6	-17
TAPA	-101	-107	-6
VICT	-17	-15	-6

Table S3: Comparative 2003 earthquake sizes for models using time series corrected for viscoelastic relaxation from a mantle using different Maxwell times (τ_m).

	τ_m = 2.5 yr	τ_m = 4 yr	τ_m = 8 yr	τ_m = 15 yr	τ_m = 25 yr	τ_m = 40 yr	no correction
M_o(10^{20} N m)	2.05	1.98	2.00	1.84	2.00	2.00	2.49
Potency (10^9 m^3)	5.13	4.95	5.00	4.60	5.00	5.00	6.23
M_w	7.5	7.5	7.5	7.4	7.5	7.5	7.5
M_o^{1995}/M_o^{2003}	4.7	4.9	4.5	5.2	4.5	4.5	4.0‡
$\%M_o^{10-40km\dagger}$	91	93	92	97	93	93	91

† Percentage of coseismic moment relased betwen depths of 10 and 40 km.

‡ 1995 coseismic moment from the model without viscoelastic relaxation corrections.

Table S4: Coseismic displacements from the 2003 Tecomán earthquake at GPS sites active during the earthquake.

	Maxwell time (τ_m) for the mantle used in the corrections for postseismic viscoelastic deformation																	
	τ_m = 2.5 yr			τ_m = 4 yr			τ_m = 8 yr			τ_m = 15 yr			τ_m = 25 yr			τ_m = 40 yr		
Site	North	East	Vert.	North	East	Vert.	North	East	Vert.	North	East	Vert.	North	East	Vert.	North	East	Vert.
	mm	mm	mm	mm	mm	mm	mm	mm	mm	mm	mm	mm	mm	mm	mm	mm	mm	mm
	±1	±1	±2	±1	±1	±2	±1	±1	±2	±1	±1	±2	±1	±1	±2	±1	±1	±2
AUTA	-41	-2	-7	-40	-2	-7	-40	-1	-7	-38	-1	-7	-40	-1	-7	-40	-1	-7
AVAL	-81	-43	-16	-80	-41	-16	-82	-42	-17	-78	-40	-18	-81	-42	-17	-81	-42	-17
AYUT	-21	-1	-2	-20	-1	-2	-21	-1	-2	-19	-1	-2	-20	-1	-2	-21	-1	-2
CEBO	-22	-14	-0	-22	-14	-0	-22	-14	-0	-21	-13	-1	-22	-14	-0	-22	-14	-0
CGUZ	-43	-26	-4	-43	-25	-4	-43	-26	-5	-41	-24	-5	-43	-25	-5	-43	-25	-5
CHAC	-3	0	-2	-3	0	-2	-3	0	-2	-3	0	-2	-3	0	-2	-3	0	-2
CHAM	-3	-2	-5	-3	-2	-5	-3	-2	-5	-2	-2	-4	-3	-2	-5	-3	-2	-5
COLI	-118	-75	-39	-116	-73	-39	-119	-75	-41	-111	-70	-41	-117	-73	-41	-118	-74	-41
COOB	-93	-55	-23	-92	-53	-23	-94	-54	-24	-89	-51	-25	-93	-54	-24	-93	-54	-24
COS2	-21	-10	0	-20	-10	0	-21	-10	-0	-20	-9	-0	-21	-10	-0	-21	-10	-0
CRIP	-74	-38	56	-71	-37	53	-76	-37	48	-70	-36	47	-75	-37	53	-75	-37	54
GUAC	-15	-1	-1	-14	-1	-1	-15	-1	-1	-14	-1	-1	-15	-1	-1	-15	-1	-1
GUFI	-33	1	-10	-31	1	-10	-31	2	-9	-28	2	-9	-31	2	-10	-31	2	-10
INEG	-4	-2	1	-4	-2	0	-4	-2	0	-4	-2	0	-4	-2	0	-4	-2	0
LIM2	-22	-9	-0	-21	-8	-0	-22	-8	-0	-21	-8	-0	-22	-8	-0	-22	-8	-0
MANZ	-91	-28	17	-88	-28	16	-91	-26	18	-84	-28	18	-90	-27	19	-89	-27	20
MCAB	-10	-3	1	-10	-3	0	-10	-3	0	-10	-3	0	-10	-3	0	-10	-3	0
MELA	-9	-15	-7	-7	-14	-6	-8	-11	-6	-6	-12	-5	-7	-13	-6	-7	-13	-6
MILN	-3	-1	-4	-3	-1	-4	-3	-0	-4	-3	-1	-3	-3	-1	-4	-3	-1	-4
MIRA	-201	-147	-11	-196	-139	2	-205	-140	5	-198	-130	17	-199	-137	15	-199	-137	14
NOVI	-82	-100	-21	-84	-96	-16	-81	-90	-14	-80	-82	-4	-83	-91	-10	-83	-91	-11
PORT	-2	-0	-2	-2	-0	-2	-2	-0	-2	-2	-0	-2	-2	-0	-2	-2	-0	-2
PURI	-23	1	-7	-22	2	-6	-22	2	-6	-20	2	-6	-22	2	-6	-22	2	-6
SEBA	-7	0	-1	-7	0	-1	-7	0	-1	-7	0	-1	-7	0	-1	-7	0	-1
SJDL	-53	1	28	-53	-5	21	-51	7	24	-48	-2	16	-54	-5	21	-53	-4	19
TAPA	-48	-17	-5	-47	-16	-5	-48	-16	-5	-46	-15	-5	-48	-16	-5	-48	-16	-5
TENA	-4	-8	-7	-3	-8	-6	-3	-7	-6	-2	-7	-6	-3	-7	-6	-3	-7	-6
UCOL	-46	-22	12	-44	-21	10	-46	-19	11	-42	-20	10	-46	-20	12	-45	-20	12
UGEO	-14	-6	1	-14	-6	0	-14	-6	0	-13	-5	0	-14	-6	0	-14	-6	0
VICT	-20	-38	-14	-21	-36	-13	-20	-32	-12	-19	-29	-9	-21	-33	-11	-21	-34	-11

Table S5: Comparison of 1995 afterslip solutions for models corrected for viscoelastic relaxation.

	τ_m = 2.5 yr	τ_m = 4 yr	τ_m = 8 yr	τ_m = 15 yr	τ_m = 25 yr	τ_m = 40 yr	no correction
$M_o(10^{20}$ N m)	5.07	6.37	8.91	10.80	12.00	11.90	13.2
Equivalent M_w	7.7	7.8	7.9	8.0	8.0	8.0	8.0
$M_o^{as}/M_o^{co}(\%)$	52	66	92	111	124	124	134
t_c (days)	5	8	11	13	14	14	82

τ_m: Mantle Maxwell time used for the viscoelastic corrections.
co: coseismic, as: afterslip, t_c: logarithmic decay constant.

Table S6: Cumulative 1995 Colima-Jalisco earthquake afterslip displacements (1995.77-2020.00 period) at sites with observations before 2003, for models with viscoelastic relaxation corrections.

	Maxwell time (τ_m) for the mantle used in the corrections for postseismic viscoelastic deformation																	
	τ_m = 2.5 yr			τ_m = 4 yr			τ_m = 8 yr			τ_m = 15 yr			τ_m = 25 yr			τ_m = 40 yr		
Site	North	East	Vert.	North	East	Vert.	North	East	Vert.	North	East	Vert.	North	East	Vert.	North	East	Vert.
	mm	mm	mm	mm	mm	mm	mm	mm	mm	mm	mm	mm	mm	mm	mm	mm	mm	mm
	±1	±1	±2	±1	±1	±2	±1	±1	±2	±1	±1	±2	±1	±1	±2	±1	±1	±2
AUTA	-94	-49	1	-135	-73	-13	-199	-109	-30	-241	-150	-37	-258	-163	-33	-262	-167	-39
AVAL	-55	-40	0	-80	-57	-13	-118	-82	-27	-137	-107	-35	-150	-118	-39	-146	-118	-37
AYUT	-76	-39	-11	-113	-58	-20	-159	-77	-28	-198	-103	-38	-215	-113	-40	-216	-114	-40
CEBO	-29	-27	-2	-41	-38	-4	-60	-52	-6	-73	-70	-10	-82	-78	-11	-80	-77	-11
CGUZ	-41	-37	-4	-59	-52	-11	-88	-73	-18	-104	-96	-25	-117	-107	-29	-113	-106	-27
CHAC	-30	-6	-11	-56	-16	-23	-89	-26	-31	-104	-38	-36	-112	-42	-38	-114	-43	-38
CHAM	-175	-101	169	-175	-129	237	-201	-157	258	-212	-185	390	-223	-192	420	-225	-194	425
COLI	-64	-31	11	-87	-42	-6	-118	-63	-14	-130	-81	-22	-136	-88	-20	-135	-90	-18
COOB	-56	-36	4	-80	-52	-12	-116	-76	-25	-132	-97	-34	-144	-108	-37	-140	-108	-34
COS2	-34	-27	-2	-47	-39	-4	-67	-52	-5	-83	-70	-8	-94	-78	-10	-91	-78	-9
CRIP	-250	-48	159	-265	-46	218	-287	-52	277	-286	-63	319	-288	-67	352	-292	-69	349
GUAC	-58	-26	-6	-86	-38	-11	-118	-50	-14	-149	-69	-20	-163	-75	-22	-162	-76	-21
GUFI	-128	-40	52	-164	-50	78	-249	-88	64	-285	-127	105	-312	-150	128	-313	-150	112
INEG	-10	-7	1	-14	-10	1	-19	-14	2	-24	-18	2	-27	-20	2	-27	-20	2
LIM2	-40	-29	-2	-56	-42	-5	-79	-57	-7	-100	-76	-11	-111	-84	-12	-109	-84	-12
LIMA	-40	-29	-2	-56	-42	-5	-79	-55	-6	-100	-75	-10	-111	-83	-12	-109	-82	-11
MANZ	-219	-50	136	-235	-48	185	-262	-66	216	-273	-84	247	-292	-101	265	-289	-94	262
MCAB	-26	-15	1	-36	-22	0	-50	-29	0	-64	-39	-0	-71	-43	-1	-70	-43	-0
MELA	-224	-88	55	-242	-48	210	-300	-29	395	-331	-76	620	-345	-84	640	-363	-85	656
MILN	-93	-65	41	-131	-96	46	-196	-128	0	-212	-169	73	-230	-185	88	-237	-188	79
MIRA	-171	-57	11	-185	-48	38	-233	-48	122	-157	-50	199	-173	-78	224	-183	-66	192
NOVI	-79	-37	-11	-84	-27	0	-114	-24	38	-80	-3	86	-62	13	132	-71	-5	109
PORT	-30	-9	-8	-74	-28	-23	-139	-45	-50	-165	-78	-59	-186	-93	-69	-190	-93	-71
PURI	-100	-42	30	-143	-64	33	-225	-105	9	-264	-139	29	-281	-159	42	-289	-161	29
SEBA	-44	-10	-6	-66	-17	-9	-92	-23	-12	-115	-34	-16	-125	-38	-18	-126	-38	-18
SJDL	-59	-23	-8	-61	2	79	-90	-5	133	-101	43	120	-107	38	129	-102	37	112
TAPA	-62	-46	-7	-88	-65	-16	-126	-89	-24	-153	-119	-34	-170	-132	-38	-167	-132	-36
TENA	-231	-49	80	-254	-56	292	-300	-80	492	-317	-149	706	-333	-164	760	-344	-158	769
TOMA	-55	-20	-5	-100	-48	-18	-170	-74	-52	-204	-117	-39	-228	-137	-43	-234	-137	-45
UCOL	-207	-86	161	-227	-76	192	-272	-72	201	-308	-76	275	-314	-102	283	-323	-95	286
UGEO	-29	-21	-0	-41	-30	-1	-58	-40	-1	-73	-53	-3	-81	-59	-4	-80	-59	-3
UMON	-31	-21	-0	-44	-30	-1	-61	-39	-2	-77	-53	-3	-86	-59	-4	-84	-58	-3
VICT	-47	-26	-15	-45	-18	-18	-67	-14	-2	-40	11	22	-41	25	38	-39	19	33

Table S7: Comparison of 2003 afterslip solutions for models corrected for viscoelastic relaxation.

	τ_m = 2.5 yr	τ_m = 4 yr	τ_m = 8 yr	τ_m = 15 yr	τ_m = 25 yr	τ_m = 40 yr	no correction
$M_o(10^{20}$ N m)	1.55	1.77	2.48	2.84	3.16	3.05	3.00
M_w	7.4	7.4	7.5	7.6	7.6	7.6	7.6
$M_o^{as}/M_o^{co}(\%)$	76	89	124	154	158	153	121
t_c (days)	11	3	7	6	16	15	64

τ_m: Mantle Maxwell time used for the viscoelastic corrections.
co: coseismic, as: afterslip, t_c: logarithmic decay constant.

Table S8: Cumulative 2003 Tecomán earthquake afterslip displacements (2003.06-2020.00 period) at sites with observations before 2005.

	Maxwell time (τ_m) for the mantle used in the corrections for postseismic viscoelastic deformation																	
	τ_m = 2.5 yr			τ_m = 4 yr			τ_m = 8 yr			τ_m = 15 yr			τ_m = 25 yr			τ_m = 40 yr		
Site	North mm ±1	East mm ±1	Vert. mm ±2	North mm ±1	East mm ±1	Vert. mm ±2	North mm ±1	East mm ±1	Vert. mm ±2	North mm ±1	East mm ±1	Vert. mm ±2	North mm ±1	East mm ±1	Vert. mm ±2	North mm ±1	East mm ±1	Vert. mm ±2
AUTA	-23	2	-2	-28	3	-3	-29	1	-2	-44	3	-6	-55	7	-8	-54	5	-7
AVAL	-28	-2	14	-46	-8	3	-64	-13	-1	-81	-21	-5	-88	-23	-3	-87	-24	-3
AYUT	-17	2	-2	-20	3	-3	-23	1	-4	-32	2	-5	-38	4	-7	-37	3	-6
CEBO	-13	-6	-1	-20	-9	-3	-32	-13	-5	-37	-16	-6	-39	-16	-6	-38	-16	-6
CGUZ	-20	-6	1	-33	-11	-4	-51	-17	-9	-59	-21	-11	-61	-21	-10	-60	-21	-10
CHAC	-4	1	-1	-5	1	-1	-6	-0	-3	-9	0	-3	-12	1	-4	-11	1	-3
CHAM	-7	1	-2	-6	-1	-3	-8	-4	-0	-14	-3	-3	-19	-2	-4	-18	-2	-4
COLI	-46	4	37	-56	-2	33	-72	-14	35	-92	-24	33	-91	-24	35	-92	-26	33
COOB	-32	1	22	-48	-6	12	-67	-14	8	-84	-23	5	-88	-25	8	-88	-26	7
COS2	-14	-5	-1	-21	-7	-2	-30	-10	-4	-36	-12	-4	-39	-13	-5	-38	-13	-5
CRIP	-66	-2	10	-58	-5	16	-52	-13	26	-56	-16	37	-50	-21	51	-49	-21	53
GUAC	-13	1	-1	-16	1	-2	-19	1	-3	-26	1	-3	-31	2	-4	-30	2	-4
GUFI	-19	0	0	-20	1	-1	-21	-3	3	-33	1	-2	-43	5	-6	-43	4	-6
INEG	-3	-1	0	-5	-2	0	-7	-3	0	-8	-4	0	-9	-4	0	-9	-4	0
LIM2	-16	-4	-1	-22	-6	-3	-31	-7	-4	-38	-9	-5	-42	-10	-6	-41	-10	-5
LIMA	-16	-4	-1	-22	-5	-2	-30	-7	-4	-37	-9	-4	-41	-9	-5	-40	-9	-5
MANZ	-67	-4	16	-63	-7	19	-57	-16	24	-66	-16	29	-61	-18	39	-61	-19	39
MCAB	-9	-2	-0	-12	-2	-0	-16	-3	-1	-19	-4	-1	-22	-4	-1	-21	-4	-1
MELA	-19	-0	-3	-10	-3	-2	-9	-9	2	-15	-8	-2	-20	-6	-6	-20	-7	-6
MILN	-6	1	-2	-6	-0	-3	-8	-3	-2	-13	-2	-4	-18	-1	-5	-16	-1	-5
MIRA	-137	-17	26	-131	-43	55	-124	-77	65	-124	-76	130	-95	-69	262	-96	-66	242
NOVI	-78	-3	25	-71	18	77	-102	-7	142	-80	33	187	-67	99	244	-66	87	228
PORT	-4	1	-1	-5	0	-2	-7	-1	-3	-11	-0	-4	-14	1	-5	-13	0	-5
PURI	-16	2	-2	-16	3	-2	-16	-1	1	-26	2	-2	-34	6	-4	-33	5	-4
SEBA	-8	2	-1	-9	2	-1	-11	1	-2	-15	2	-2	-18	3	-3	-17	3	-3
SJDL	-78	7	15	-67	42	93	-102	29	181	-110	79	162	-110	76	129	-110	78	136
TAPA	-26	-5	-2	-38	-6	-6	-48	-6	-8	-64	-10	-11	-73	-10	-13	-70	-11	-12
TENA	-12	1	-3	-7	-2	-4	-8	-6	-1	-15	-5	-4	-20	-3	-7	-20	-4	-6
TOMA	-5	2	-1	-6	1	-2	-8	-2	-3	-12	-1	-4	-16	1	-4	-15	0	-4
UCOL	-45	-4	10	-37	-6	12	-33	-12	19	-40	-11	18	-40	-10	18	-40	-11	17
UGEO	-11	-3	-0	-15	-4	-1	-22	-6	-2	-26	-7	-2	-29	-8	-2	-28	-8	-2
UMON	-11	-3	-0	-15	-4	-1	-21	-5	-2	-26	-6	-2	-29	-7	-2	-28	-7	-2
VICT	-31	4	5	-34	27	32	-57	27	73	-45	60	91	-48	81	105	-47	77	98

Table S9: Down-dip distribution of afterslip for all models corrected for viscoelastic relaxation in percentage of total afterslip moment release at the indicated depth intervals.

τ_m	1995 afterslip depth intervals				2003 afterslip depth intervals			
(years)	$0-15$ km	$15-40$ km	$40-60$ km	below 60 km	$0-15$ km	$15-40$ km	$40-60$ km	below 60 km
2	43	37	15	4	39	31	18	11
4	19	58	19	4	10	52	27	12
8	18	62	17	3	7	54	28	12
15	12	64	19	4	4	57	27	12
25	11	64	20	5	6	54	23	17
40	12	64	19	4	6	55	23	16
no correction	13	59	21	7	11	50	21	18

τ_m: Mantle Maxwell time used for the viscoelastic relaxation corrections.

Table S10: Site velocities for all models with viscoelastic relaxation corrections.[†]

Site	Maxwell time (τ_m) for the mantle used in the corrections for postseismic viscoelastic deformation								
	τ_m = 2.5 yr			τ_m = 4 yr			τ_m = 8 yr		
	North (mm/yr)	East (mm/yr)	Vert. (mm/yr)	North (mm/yr)	East (mm/yr)	Vert. (mm/yr)	North (mm/yr)	East (mm/yr)	Vert. (mm/yr)
ANIG	3.6 ± 0.9	2.0 ± 0.9	−3.8 ± 1.5	4.6 ± 0.9	2.3 ± 0.9	−3.2 ± 1.5	5.4 ± 0.9	2.2 ± 0.9	−2.6 ± 1.5
AUTA	8.4 ± 0.8	5.3 ± 0.8	4.7 ± 1.8	10.5 ± 0.8	6.3 ± 0.8	5.2 ± 1.8	11.2 ± 0.8	6.6 ± 0.8	4.9 ± 1.8
AVAL	5.7 ± 3.4	6.5 ± 1.1	3.3 ± 4.9	6.9 ± 3.4	6.8 ± 1.1	4.6 ± 4.9	8.3 ± 3.4	6.8 ± 1.1	5.5 ± 4.9
AYUT	7.6 ± 0.8	4.8 ± 0.8	2.9 ± 1.8	8.9 ± 0.8	5.1 ± 0.8	3.5 ± 1.8	8.8 ± 0.8	4.4 ± 0.8	3.8 ± 1.8
CALC	16.1 ± 1.3	10.1 ± 1.3	−9.2 ± 2.1	16.3 ± 1.3	9.9 ± 1.3	−9.8 ± 2.1	16.4 ± 1.3	9.7 ± 1.3	−10.3 ± 2.1
CEBO	6.7 ± 0.9	3.9 ± 0.9	−4.3 ± 4.2	6.5 ± 0.9	3.8 ± 0.9	−3.5 ± 4.2	6.4 ± 0.9	3.1 ± 0.9	−2.8 ± 4.2
CGUZ	7.3 ± 0.9	4.7 ± 0.9	0.3 ± 2.0	7.9 ± 0.9	5.1 ± 0.9	1.1 ± 2.0	8.2 ± 0.9	4.8 ± 0.9	1.8 ± 2.0
CHAC	7.0 ± 0.8	4.8 ± 0.8	−1.4 ± 4.2	7.8 ± 0.8	4.4 ± 0.8	−2.1 ± 4.2	8.2 ± 0.8	3.7 ± 0.8	−2.8 ± 4.2
CHAM	6.8 ± 0.8	6.7 ± 0.8	14.2 ± 3.2	8.6 ± 0.8	8.1 ± 0.8	9.9 ± 3.2	11.7 ± 0.8	9.0 ± 0.8	6.1 ± 3.2
CHMC	8.4 ± 1.1	5.7 ± 1.1	−0.8 ± 1.8	9.1 ± 1.1	6.5 ± 1.1	−0.3 ± 1.8	11.1 ± 1.1	7.5 ± 1.1	−0.6 ± 1.8
COJB	7.9 ± 1.6	1.0 ± 1.6	5.0 ± 5.9	9.3 ± 1.6	2.1 ± 1.6	5.7 ± 5.9	10.8 ± 1.6	3.4 ± 1.6	5.9 ± 5.9
COLI	9.0 ± 0.6	5.0 ± 0.6	1.1 ± 0.9	10.1 ± 0.6	6.2 ± 0.6	1.9 ± 0.9	11.5 ± 0.6	7.5 ± 0.6	1.8 ± 0.9
COLW	6.1 ± 1.8	4.5 ± 1.8	−3.0 ± 3.1	7.7 ± 1.8	5.7 ± 1.8	−2.2 ± 3.1	9.4 ± 1.8	7.0 ± 1.8	−1.9 ± 3.1
COOB	9.0 ± 0.8	4.9 ± 0.8	3.0 ± 1.2	10.4 ± 0.8	6.2 ± 0.8	3.8 ± 1.2	11.7 ± 0.8	7.2 ± 0.8	3.8 ± 1.2
COPE	6.8 ± 1.8	4.1 ± 1.8	−2.5 ± 3.2	8.3 ± 1.8	5.3 ± 1.8	−1.8 ± 3.2	9.8 ± 1.8	6.6 ± 1.8	−1.6 ± 3.2
COPN	6.2 ± 1.8	4.6 ± 1.8	−1.5 ± 3.3	7.8 ± 1.8	5.8 ± 1.8	−0.8 ± 3.3	9.4 ± 1.8	7.1 ± 1.8	−0.6 ± 3.3
COS2	7.1 ± 0.9	5.0 ± 0.9	−6.9 ± 4.3	7.0 ± 0.9	5.0 ± 0.9	−6.0 ± 4.3	6.3 ± 0.9	4.0 ± 0.9	−5.4 ± 4.3
CRIP	10.1 ± 1.1	1.1 ± 1.1	9.3 ± 3.9	12.2 ± 1.1	2.0 ± 1.1	1.4 ± 3.9	14.4 ± 1.1	3.4 ± 1.1	−7.2 ± 3.9
CUVA	5.1 ± 1.0	1.6 ± 1.0	—	6.4 ± 1.0	2.3 ± 1.0	—	7.6 ± 1.0	2.9 ± 1.0	—
FARO	12.6 ± 1.6	5.1 ± 1.6	−8.6 ± 2.7	13.0 ± 1.6	5.8 ± 1.6	−9.4 ± 2.7	14.4 ± 1.6	6.3 ± 1.6	−11.3 ± 2.7
GUAC	6.2 ± 0.8	4.2 ± 0.8	−0.2 ± 1.7	6.8 ± 0.8	4.0 ± 0.8	0.6 ± 1.7	6.1 ± 0.8	3.1 ± 0.8	1.1 ± 1.7
GUFI	7.8 ± 0.8	4.0 ± 0.8	10.1 ± 3.6	10.1 ± 0.8	4.7 ± 0.8	9.3 ± 3.6	12.6 ± 0.8	5.6 ± 0.8	8.4 ± 3.6
IITJ	6.7 ± 1.6	2.5 ± 1.6	−3.5 ± 2.8	6.8 ± 1.6	2.7 ± 1.6	−2.6 ± 2.8	6.1 ± 1.6	2.3 ± 1.6	−1.9 ± 2.8
INEG	5.2 ± 0.6	2.3 ± 0.6	—	5.2 ± 0.6	2.4 ± 0.6	—	4.8 ± 0.6	2.1 ± 0.6	—
LIM2	7.5 ± 1.1	4.9 ± 1.1	−9.7 ± 6.5	7.8 ± 1.1	5.0 ± 1.1	−8.8 ± 6.5	7.1 ± 1.1	4.1 ± 1.1	−8.1 ± 6.5
LIMA	9.0 ± 3.4	3.1 ± 3.8	1.1 ± 20.1	6.2 ± 3.4	0.2 ± 3.8	1.8 ± 20.1	4.2 ± 3.4	−2.9 ± 3.8	2.0 ± 20.1
LZCR	13.8 ± 1.3	9.0 ± 1.3	0.2 ± 2.1	13.9 ± 1.3	8.9 ± 1.3	0.1 ± 2.1	13.7 ± 1.3	8.8 ± 1.3	0.1 ± 2.1
MANZ	9.8 ± 1.1	3.6 ± 1.1	4.8 ± 1.9	11.2 ± 1.1	5.1 ± 1.1	3.5 ± 1.9	12.6 ± 1.1	6.9 ± 1.1	0.9 ± 1.9
MASC	4.1 ± 1.0	3.1 ± 1.0	−1.5 ± 1.6	5.3 ± 1.0	3.5 ± 1.0	−1.4 ± 1.6	6.6 ± 1.0	3.6 ± 1.0	−1.2 ± 1.6
MCAB	6.5 ± 1.1	4.8 ± 1.1	−1.8 ± 5.2	5.7 ± 1.1	4.0 ± 1.1	−1.2 ± 5.2	4.3 ± 1.1	2.7 ± 1.1	−0.8 ± 5.2
MELA	6.8 ± 0.8	7.1 ± 0.8	8.9 ± 3.6	8.6 ± 0.8	7.2 ± 0.8	5.1 ± 3.6	12.7 ± 0.8	7.9 ± 0.8	−1.4 ± 3.6
MILN	4.5 ± 1.0	4.8 ± 1.0	6.4 ± 4.2	6.6 ± 1.0	6.0 ± 1.0	6.0 ± 4.2	9.3 ± 1.0	6.7 ± 1.0	4.6 ± 4.2
MIRA	12.2 ± 1.3	3.0 ± 1.3	14.9 ± 6.4	12.4 ± 1.3	7.3 ± 1.3	7.1 ± 6.4	13.6 ± 1.3	14.0 ± 1.3	2.9 ± 6.4
MMIG	10.1 ± 1.0	5.0 ± 1.0	−4.0 ± 1.6	10.3 ± 1.0	5.2 ± 1.0	−4.7 ± 1.6	11.0 ± 1.0	5.3 ± 1.0	−5.9 ± 1.6
MNZO	9.5 ± 2.0	6.4 ± 2.0	−3.1 ± 3.5	9.9 ± 2.0	6.9 ± 2.0	−2.0 ± 3.5	11.7 ± 2.0	8.2 ± 2.0	−1.4 ± 3.5
MPR1	3.9 ± 0.9	2.7 ± 0.9	−1.2 ± 1.4	4.6 ± 0.9	2.9 ± 0.9	−1.4 ± 1.4	5.2 ± 0.9	2.7 ± 0.9	−1.6 ± 1.4
NOVI	16.9 ± 1.3	9.3 ± 1.4	3.6 ± 7.4	16.3 ± 4.4	6.0 ± 1.4	−5.8 ± 7.4	20.2 ± 4.4	9.2 ± 1.4	−17.2 ± 7.4
NVDO	8.5 ± 1.0	5.0 ± 1.0	3.3 ± 1.6	10.1 ± 1.0	6.3 ± 1.0	3.9 ± 1.6	11.3 ± 1.0	7.4 ± 1.0	4.1 ± 1.6
PENA	8.0 ± 0.9	4.6 ± 0.9	−1.2 ± 2.9	9.6 ± 0.9	5.6 ± 0.9	0.2 ± 2.9	11.8 ± 0.9	7.1 ± 0.9	0.8 ± 2.9
PORT	7.3 ± 1.6	3.9 ± 1.6	12.9 ± 4.9	9.1 ± 1.6	4.2 ± 1.6	11.2 ± 4.9	10.9 ± 1.6	4.0 ± 1.6	8.9 ± 4.9
PURI	5.0 ± 0.7	3.6 ± 0.7	3.9 ± 1.2	7.1 ± 0.7	4.7 ± 0.7	4.6 ± 1.2	10.0 ± 0.7	5.9 ± 0.7	4.8 ± 1.2
PZUL	6.3 ± 1.1	4.2 ± 1.1	2.5 ± 1.9	7.5 ± 1.1	4.5 ± 1.1	2.6 ± 1.9	8.8 ± 1.1	4.6 ± 1.1	1.5 ± 1.9
SEBA	4.7 ± 0.8	4.4 ± 0.8	−3.2 ± 2.1	5.4 ± 0.8	4.0 ± 0.8	−2.8 ± 2.1	5.2 ± 0.8	3.1 ± 0.8	−2.2 ± 2.1
SJDL	14.7 ± 0.9	9.7 ± 0.9	−1.6 ± 3.9	14.2 ± 0.9	6.6 ± 0.9	−13.6 ± 3.9	17.9 ± 0.9	7.3 ± 0.9	−25.5 ± 3.9
TAPA	6.8 ± 0.9	5.4 ± 0.9	1.4 ± 4.1	7.9 ± 0.9	5.8 ± 0.9	2.3 ± 4.1	8.1 ± 0.9	5.1 ± 0.9	2.6 ± 4.1
TECO	10.2 ± 0.9	5.8 ± 0.9	0.7 ± 1.4	10.7 ± 0.9	6.6 ± 0.9	0.9 ± 1.4	12.2 ± 0.9	8.2 ± 0.9	−0.1 ± 1.4
TENA	6.8 ± 1.4	3.6 ± 1.4	10.2 ± 3.7	8.7 ± 1.4	5.0 ± 1.4	6.2 ± 3.7	12.9 ± 1.4	7.0 ± 1.4	0.1 ± 3.7
TNCC	9.5 ± 1.7	4.7 ± 1.7	−0.3 ± 3.0	9.8 ± 1.7	5.0 ± 1.7	−0.2 ± 3.0	10.4 ± 1.7	5.3 ± 1.7	−0.5 ± 3.0
TNCM	9.1 ± 1.5	6.3 ± 1.5	−0.8 ± 2.5	9.2 ± 1.5	6.8 ± 1.5	0.0 ± 2.5	10.5 ± 1.5	7.6 ± 1.5	0.6 ± 2.5
TNCT	10.2 ± 2.5	5.1 ± 2.5	1.0 ± 4.4	10.5 ± 2.5	5.5 ± 2.5	2.3 ± 4.4	11.8 ± 2.5	6.1 ± 2.5	3.2 ± 4.4
TNLC	6.3 ± 1.7	5.1 ± 1.7	−0.0 ± 3.0	7.1 ± 1.7	5.6 ± 1.7	1.0 ± 3.0	9.3 ± 1.7	6.8 ± 1.7	1.9 ± 3.0
TNMR	11.8 ± 1.5	5.9 ± 1.5	−4.7 ± 2.5	11.9 ± 1.5	6.0 ± 1.5	−4.8 ± 2.5	12.5 ± 1.5	6.2 ± 1.5	−5.6 ± 2.5
TNMZ	10.6 ± 1.8	7.8 ± 1.8	−5.0 ± 3.1	10.7 ± 1.8	8.0 ± 1.8	−3.7 ± 3.1	12.1 ± 1.8	8.8 ± 1.8	−2.6 ± 3.1
TNTM	13.0 ± 2.2	8.4 ± 2.2	3.9 ± 4.0	12.8 ± 2.2	8.2 ± 2.2	4.1 ± 4.0	13.9 ± 2.2	8.6 ± 2.2	4.1 ± 4.0
TNZA	−1.1 ± 2.2	−2.1 ± 2.2	—	−0.7 ± 2.2	−1.6 ± 2.2	—	−0.6 ± 2.2	−1.1 ± 2.2	—
TOMA	0.7 ± 5.9	−6.2 ± 6.3	20.8 ± 36.5	5.2 ± 5.9	−5.7 ± 6.3	17.0 ± 36.5	14.6 ± 5.9	−4.9 ± 6.3	17.7 ± 36.5
UAGU	3.1 ± 1.0	3.7 ± 1.0	—	3.5 ± 1.0	4.0 ± 1.0	—	3.4 ± 1.0	3.9 ± 1.0	—
UCOL	8.5 ± 0.8	6.1 ± 0.8	−1.3 ± 1.4	9.4 ± 0.8	6.8 ± 0.8	−0.3 ± 1.4	11.9 ± 0.8	8.0 ± 0.8	−0.4 ± 1.4
UGEO	5.2 ± 0.7	2.3 ± 0.7	−2.9 ± 1.1	6.0 ± 0.7	2.9 ± 0.7	−2.2 ± 1.1	6.3 ± 0.7	3.1 ± 0.7	−1.5 ± 1.1
UMON	9.4 ± 2.0	7.1 ± 2.0	0.0 ± 17.9	7.1 ± 2.0	5.1 ± 2.0	0.6 ± 17.9	4.7 ± 2.0	2.6 ± 2.0	0.9 ± 17.9
VALL	5.1 ± 3.1	−6.7 ± 3.1	−0.2 ± 5.9	5.8 ± 3.1	−6.4 ± 3.1	−0.4 ± 5.9	6.5 ± 3.1	−6.5 ± 3.1	−0.7 ± 5.9
VICT	12.8 ± 0.9	11.1 ± 0.9	4.5 ± 3.7	12.5 ± 0.9	8.6 ± 0.9	1.4 ± 3.7	14.3 ± 0.9	7.8 ± 0.9	−3.5 ± 3.7

Table S1.10: Continued from previous page.

Site	Maxwell time (τ_m) for the mantle used in the corrections for postseismic viscoelastic deformation								
	τ_m = 15 yr			τ_m = 25 yr			τ_m = 40 yr		
	North (mm/yr)	East (mm/yr)	Vert. (mm/yr)	North (mm/yr)	East (mm/yr)	Vert. (mm/yr)	North (mm/yr)	East (mm/yr)	Vert. (mm/yr)
ANIG	5.2 ± 0.9	1.8 ± 0.9	-2.2 ± 1.5	4.9 ± 0.9	1.6 ± 0.9	-2.0 ± 1.5	4.4 ± 0.9	1.4 ± 0.9	-2.0 ± 1.5
AUTA	11.4 ± 0.8	6.0 ± 0.8	4.9 ± 1.8	11.4 ± 0.8	5.0 ± 0.8	4.5 ± 1.8	10.3 ± 0.8	4.4 ± 0.8	4.4 ± 1.8
AVAL	8.7 ± 3.4	7.0 ± 1.1	6.1 ± 4.9	9.1 ± 3.4	6.9 ± 1.1	6.0 ± 4.9	8.2 ± 3.4	6.3 ± 1.1	5.7 ± 4.9
AYUT	8.3 ± 0.8	3.6 ± 0.8	4.1 ± 1.8	7.8 ± 0.8	2.8 ± 0.8	4.2 ± 1.8	6.6 ± 0.8	2.2 ± 0.8	4.1 ± 1.8
CALC	16.1 ± 1.3	9.8 ± 1.3	-10.5 ± 2.1	16.1 ± 1.3	9.8 ± 1.3	-10.6 ± 2.1	15.9 ± 1.3	9.9 ± 1.3	-10.6 ± 2.1
CEBO	6.0 ± 0.9	2.6 ± 0.9	-2.5 ± 4.2	5.8 ± 0.9	2.2 ± 0.9	-2.3 ± 4.2	5.1 ± 0.9	1.5 ± 0.9	-2.4 ± 4.2
CGUZ	7.7 ± 0.9	4.2 ± 0.9	2.2 ± 2.0	7.3 ± 0.9	3.6 ± 0.9	2.1 ± 2.0	6.5 ± 0.9	2.9 ± 0.9	1.9 ± 2.0
CHAC	8.2 ± 0.8	3.4 ± 0.8	-3.2 ± 4.2	8.2 ± 0.8	3.2 ± 0.8	-3.4 ± 4.2	7.9 ± 0.8	3.0 ± 0.8	-3.6 ± 4.2
CHAM	13.2 ± 0.8	9.3 ± 0.8	-1.9 ± 3.2	14.2 ± 0.8	8.9 ± 0.8	-4.3 ± 3.2	14.2 ± 0.8	8.6 ± 0.8	-5.3 ± 3.2
CHMC	12.3 ± 1.1	7.9 ± 1.1	-2.8 ± 1.8	13.0 ± 1.1	7.7 ± 1.1	-3.8 ± 1.8	13.0 ± 1.1	7.4 ± 1.1	-4.4 ± 1.8
COJB	10.7 ± 1.6	3.7 ± 1.6	6.0 ± 5.9	10.5 ± 1.6	3.5 ± 1.6	5.8 ± 5.9	9.9 ± 1.6	3.1 ± 1.6	5.6 ± 5.9
COLI	11.6 ± 0.6	7.8 ± 0.6	1.6 ± 0.9	11.6 ± 0.6	7.8 ± 0.6	1.1 ± 0.9	11.1 ± 0.6	7.5 ± 0.6	1.0 ± 0.9
COLW	9.3 ± 1.8	7.3 ± 1.8	-1.9 ± 3.1	9.2 ± 1.8	7.2 ± 1.8	-2.1 ± 3.1	8.5 ± 1.8	6.7 ± 1.8	-2.3 ± 3.1
COOB	11.5 ± 0.8	7.4 ± 0.8	3.6 ± 1.2	11.5 ± 0.8	7.2 ± 0.8	3.1 ± 1.2	10.8 ± 0.8	6.7 ± 0.8	2.9 ± 1.2
COPE	9.7 ± 1.8	6.8 ± 1.8	-1.6 ± 3.2	9.5 ± 1.8	6.7 ± 1.8	-1.8 ± 3.2	8.9 ± 1.8	6.2 ± 1.8	-1.9 ± 3.2
COPN	9.3 ± 1.8	7.4 ± 1.8	-0.5 ± 3.3	9.2 ± 1.8	7.2 ± 1.8	-0.7 ± 3.3	8.5 ± 1.8	6.8 ± 1.8	-0.9 ± 3.3
COS2	5.6 ± 0.9	3.2 ± 0.9	-5.0 ± 4.3	5.2 ± 0.9	2.6 ± 0.9	-5.0 ± 4.3	4.5 ± 0.9	1.9 ± 0.9	-5.0 ± 4.3
CRIP	13.4 ± 1.1	4.6 ± 1.1	-13.1 ± 3.9	13.3 ± 1.1	5.0 ± 1.1	-17.6 ± 3.9	13.4 ± 1.1	5.3 ± 1.1	-17.9 ± 3.9
CUVA	7.5 ± 1.0	2.8 ± 1.0	—	7.2 ± 1.0	2.4 ± 1.0	—	6.5 ± 1.0	2.0 ± 1.0	—
FARO	13.5 ± 1.6	6.8 ± 1.6	-10.2 ± 2.7	13.5 ± 1.6	7.1 ± 1.6	-10.2 ± 2.7	13.4 ± 1.6	7.3 ± 1.6	-10.2 ± 2.7
GUAC	5.5 ± 0.8	2.5 ± 0.8	1.5 ± 1.7	5.0 ± 0.8	1.9 ± 0.8	1.6 ± 1.7	3.8 ± 0.8	1.4 ± 0.8	1.6 ± 1.7
GUFI	13.3 ± 0.8	5.4 ± 0.8	6.8 ± 3.6	14.1 ± 0.8	4.8 ± 0.8	6.0 ± 3.6	13.2 ± 0.8	4.3 ± 0.8	6.1 ± 3.6
IITJ	5.0 ± 1.6	1.6 ± 1.6	-1.7 ± 2.8	4.7 ± 1.6	1.0 ± 1.6	-1.5 ± 2.8	3.8 ± 1.6	0.5 ± 1.6	-1.5 ± 2.8
INEG	4.3 ± 0.6	1.7 ± 0.6	—	4.0 ± 0.6	1.4 ± 0.6	—	3.7 ± 0.6	1.2 ± 0.6	—
LIM2	6.4 ± 1.1	3.2 ± 1.1	-7.7 ± 6.5	6.0 ± 1.1	2.5 ± 1.1	-7.6 ± 6.5	5.1 ± 1.1	1.9 ± 1.1	-7.7 ± 6.5
LIMA	4.3 ± 3.4	-3.1 ± 3.8	2.5 ± 20.1	4.5 ± 3.4	-3.4 ± 3.8	2.6 ± 20.1	3.5 ± 3.4	-4.2 ± 3.8	2.5 ± 20.1
LZCR	13.4 ± 1.3	8.9 ± 1.3	0.1 ± 2.1	13.3 ± 1.3	9.0 ± 1.3	0.2 ± 2.1	13.2 ± 1.3	9.1 ± 1.3	0.2 ± 2.1
MANZ	12.7 ± 1.1	7.8 ± 1.1	-1.7 ± 1.9	12.8 ± 1.1	8.3 ± 1.1	-4.0 ± 1.9	12.5 ± 1.1	8.1 ± 1.1	-4.4 ± 1.9
MASC	6.8 ± 1.0	3.3 ± 1.0	-1.0 ± 1.6	6.5 ± 1.0	2.9 ± 1.0	-0.9 ± 1.6	6.0 ± 1.0	2.7 ± 1.0	-0.9 ± 1.6
MCAB	3.7 ± 1.1	2.1 ± 1.1	-0.6 ± 5.2	3.4 ± 1.1	1.7 ± 1.1	-0.6 ± 5.2	2.7 ± 1.1	1.3 ± 1.1	-0.6 ± 5.2
MELA	15.0 ± 0.8	9.4 ± 0.8	-8.6 ± 3.6	16.3 ± 0.8	9.6 ± 0.8	-9.6 ± 3.6	16.9 ± 0.8	9.7 ± 0.8	-10.6 ± 3.6
MILN	10.4 ± 1.0	6.6 ± 1.0	1.6 ± 4.2	11.2 ± 1.0	6.1 ± 1.0	0.2 ± 4.2	11.1 ± 1.0	5.7 ± 1.0	-0.4 ± 4.2
MIRA	10.9 ± 1.3	12.7 ± 1.3	-12.3 ± 6.4	5.6 ± 4.3	12.5 ± 1.3	-33.9 ± 6.4	5.8 ± 4.3	11.9 ± 1.3	-30.4 ± 6.4
MMIG	10.7 ± 1.0	5.7 ± 1.0	-5.8 ± 1.6	10.7 ± 1.0	5.8 ± 1.0	-6.0 ± 1.6	10.6 ± 1.0	5.9 ± 1.0	-6.1 ± 1.6
MNZO	12.8 ± 2.0	8.8 ± 2.0	-2.1 ± 3.5	13.3 ± 2.0	9.2 ± 2.0	-2.7 ± 3.5	13.3 ± 2.0	9.2 ± 2.0	-2.9 ± 3.5
MPR1	5.2 ± 0.9	2.3 ± 0.9	-1.5 ± 1.4	5.0 ± 0.9	2.0 ± 0.9	-1.4 ± 1.4	4.7 ± 0.9	1.8 ± 0.9	-1.4 ± 1.4
NOVI	15.4 ± 1.3	1.8 ± 1.4	-27.1 ± 7.4	12.9 ± 1.3	-6.6 ± 1.4	-34.9 ± 7.4	12.6 ± 1.3	-4.7 ± 1.4	-32.2 ± 7.4
NVDO	10.8 ± 1.0	7.5 ± 1.0	4.1 ± 1.6	10.6 ± 1.0	7.2 ± 1.0	3.9 ± 1.6	9.9 ± 1.0	6.6 ± 1.0	3.7 ± 1.6
PENA	12.5 ± 0.9	7.6 ± 0.9	0.7 ± 2.9	13.0 ± 0.9	7.5 ± 0.9	0.5 ± 2.9	12.4 ± 0.9	7.2 ± 0.9	0.3 ± 2.9
PORT	11.8 ± 1.6	3.9 ± 1.6	7.3 ± 4.9	12.3 ± 1.6	3.7 ± 1.6	6.5 ± 4.9	12.1 ± 1.6	3.4 ± 1.6	5.8 ± 4.9
PURI	10.9 ± 0.7	5.9 ± 0.7	4.2 ± 1.2	10.9 ± 0.7	5.5 ± 0.7	3.8 ± 1.2	10.4 ± 0.7	5.1 ± 0.7	3.7 ± 1.2
PZUL	9.0 ± 1.1	4.4 ± 1.1	0.3 ± 1.9	9.2 ± 1.1	4.2 ± 1.1	-0.3 ± 1.9	9.0 ± 1.1	4.0 ± 1.1	-0.8 ± 1.9
SEBA	4.6 ± 0.8	2.6 ± 0.8	-1.9 ± 2.1	4.2 ± 0.8	2.2 ± 0.8	-1.8 ± 2.1	3.4 ± 0.8	2.0 ± 0.8	-1.7 ± 2.1
SJDL	18.7 ± 0.9	1.9 ± 3.0	-22.9 ± 3.9	19.0 ± 0.9	3.3 ± 3.0	-20.6 ± 3.9	18.5 ± 0.9	3.2 ± 3.0	-20.3 ± 3.9
TAPA	8.2 ± 0.9	4.8 ± 0.9	3.2 ± 4.1	8.3 ± 0.9	4.2 ± 0.9	3.2 ± 4.1	7.2 ± 0.9	3.5 ± 0.9	3.0 ± 4.1
TECO	12.1 ± 0.9	8.4 ± 0.9	-1.1 ± 1.4	11.4 ± 0.9	8.0 ± 0.9	-3.6 ± 1.4	11.4 ± 0.9	8.1 ± 0.9	-3.1 ± 1.4
TENA	15.8 ± 1.4	8.8 ± 1.4	-5.8 ± 3.7	17.8 ± 1.4	8.9 ± 1.4	-7.4 ± 3.7	18.3 ± 1.4	8.9 ± 1.4	-8.2 ± 3.7
TNCC	10.0 ± 1.7	5.1 ± 1.7	-0.9 ± 3.0	9.9 ± 1.7	4.9 ± 1.7	-1.2 ± 3.0	9.7 ± 1.7	4.9 ± 1.7	-1.2 ± 3.0
TNCM	11.6 ± 1.5	8.1 ± 1.5	-0.7 ± 2.5	12.2 ± 1.5	8.1 ± 1.5	-1.5 ± 2.5	12.4 ± 1.5	7.9 ± 1.5	-2.0 ± 2.5
TNCT	12.7 ± 2.5	6.6 ± 2.5	2.0 ± 4.4	13.2 ± 2.5	6.6 ± 2.5	1.1 ± 4.4	13.4 ± 2.5	6.4 ± 2.5	0.6 ± 4.4
TNLC	10.6 ± 1.7	7.4 ± 1.7	1.6 ± 3.0	11.1 ± 1.7	7.4 ± 1.7	1.3 ± 3.0	10.8 ± 1.7	7.2 ± 1.7	1.2 ± 3.0
TNMR	12.3 ± 1.5	6.4 ± 1.5	-5.7 ± 2.5	12.3 ± 1.5	6.5 ± 1.5	-5.8 ± 2.5	12.2 ± 1.5	6.6 ± 1.5	-5.9 ± 2.5
TNMZ	13.4 ± 1.8	9.3 ± 1.8	-3.2 ± 3.1	14.0 ± 1.8	9.7 ± 1.8	-3.5 ± 3.1	14.2 ± 1.8	9.7 ± 1.8	-3.8 ± 3.1
TNTM	15.3 ± 2.2	9.5 ± 2.2	2.6 ± 4.0	16.1 ± 2.2	9.8 ± 2.2	2.1 ± 4.0	16.6 ± 2.2	9.9 ± 2.2	1.8 ± 4.0
TNZA	-1.0 ± 2.2	-1.2 ± 2.2	—	-1.2 ± 2.2	-1.4 ± 2.2	—	-1.4 ± 2.2	-1.7 ± 2.2	—
TOMA	19.2 ± 5.9	1.3 ± 6.3	12.5 ± 36.5	23.0 ± 5.9	4.3 ± 6.3	12.1 ± 36.5	23.7 ± 5.9	3.8 ± 6.3	11.7 ± 36.5
UAGU	3.0 ± 1.0	3.6 ± 1.0	—	2.7 ± 1.0	3.4 ± 1.0	—	2.5 ± 1.0	3.2 ± 1.0	—
UCOL	13.3 ± 0.8	8.3 ± 0.8	-1.8 ± 2.7	13.9 ± 0.8	8.7 ± 0.8	-2.4 ± 2.7	13.9 ± 0.8	8.6 ± 0.8	-2.8 ± 2.7
UGEO	5.8 ± 0.7	2.8 ± 0.7	-1.2 ± 1.1	5.4 ± 0.7	2.4 ± 0.7	-1.0 ± 1.1	4.8 ± 0.7	2.0 ± 0.7	-1.0 ± 1.1
UMON	3.9 ± 2.0	1.8 ± 2.0	1.1 ± 17.9	3.5 ± 2.0	1.3 ± 2.0	1.1 ± 17.9	2.7 ± 2.0	0.7 ± 2.0	1.1 ± 17.9
VALL	6.5 ± 3.1	-6.9 ± 3.1	-0.6 ± 5.9	6.3 ± 3.1	-7.2 ± 3.1	-0.5 ± 5.9	6.0 ± 3.1	-7.4 ± 3.1	-0.5 ± 5.9
VICT	11.2 ± 0.9	3.2 ± 0.9	-7.1 ± 3.7	11.2 ± 0.9	1.5 ± 0.9	-8.7 ± 3.7	10.8 ± 0.9	2.1 ± 0.9	-8.0 ± 3.7

† Velocities are relative to the North America plate and, as described in section 1.2.1, were converted from IGS14/ITRF14 to the North America plate frame of reference using the angular velocity 7.45°N, 92.04°E, 0.183°/ Myr.

Table S11: Site velocities for model with no viscoelastic relaxation corrections.†

Site	North (mm/yr)	East (mm/yr)	Vertical (mm/yr)
ANIG	3.5 ± 0.9	1.1 ± 0.9	-1.9 ± 1.5
AUTA	9.9 ± 0.8	3.8 ± 0.8	3.6 ± 1.8
AVAL	8.4 ± 3.4	5.7 ± 1.1	5.2 ± 4.9
AYUT	6.2 ± 0.8	2.0 ± 0.8	4.3 ± 1.8
CALC	15.9 ± 1.3	10.0 ± 1.3	-10.6 ± 2.1
CEBO	5.2 ± 0.9	1.0 ± 0.9	-2.2 ± 4.2
CGUZ	7.1 ± 0.9	2.7 ± 0.9	2.2 ± 2.0
CHAC	8.9 ± 0.8	3.9 ± 0.8	-3.2 ± 4.2
CHAM	17.0 ± 0.8	10.1 ± 0.8	-12.1 ± 3.2
CHMC	14.2 ± 1.1	7.6 ± 1.1	-8.5 ± 1.8
COJB	9.2 ± 1.6	2.2 ± 1.6	5.2 ± 5.9
COLI	10.9 ± 0.6	6.8 ± 0.6	-0.4 ± 0.9
COLW	7.8 ± 1.8	5.8 ± 1.8	-2.9 ± 3.1
COOB	10.6 ± 0.8	6.0 ± 0.8	1.8 ± 1.2
COPE	8.2 ± 1.8	5.3 ± 1.8	-2.4 ± 3.2
COPN	7.8 ± 1.8	5.8 ± 1.8	-1.4 ± 3.3
COS2	4.7 ± 0.9	1.7 ± 0.9	-4.8 ± 4.3
CRIP	15.8 ± 1.1	7.7 ± 1.1	-31.3 ± 3.9
CUVA	5.5 ± 1.0	1.3 ± 1.0	—
FARO	13.8 ± 1.6	7.5 ± 1.6	-10.6 ± 2.7
GUAC	3.5 ± 0.8	1.3 ± 0.8	1.8 ± 1.7
GUFI	13.4 ± 0.8	3.3 ± 0.8	2.6 ± 3.6
IITJ	3.4 ± 1.6	-0.1 ± 1.6	-1.5 ± 2.8
INEG	3.4 ± 0.6	0.9 ± 0.6	—
LIM2	5.1 ± 1.1	1.6 ± 1.1	-7.5 ± 6.5
LIMA	5.7 ± 3.4	-3.0 ± 3.8	3.1 ± 20.1
LZCR	13.2 ± 1.3	9.1 ± 1.3	0.3 ± 2.1
MANZ	14.1 ± 1.1	9.1 ± 1.1	-11.7 ± 1.9
MASC	5.0 ± 1.0	2.4 ± 1.0	-0.8 ± 1.6
MCAB	2.5 ± 1.1	1.1 ± 1.1	-0.5 ± 5.2
MELA	17.9 ± 0.8	9.9 ± 0.8	-18.0 ± 3.6
MILN	12.5 ± 1.0	6.5 ± 1.0	-3.9 ± 4.2
MIRA	9.4 ± 1.3	8.4 ± 1.3	-33.6 ± 6.4
MMIG	10.7 ± 1.0	6.0 ± 1.0	-6.3 ± 1.6
MNZO	13.9 ± 2.0	9.7 ± 2.0	-6.2 ± 3.5
MPR1	4.3 ± 0.9	1.8 ± 0.9	-1.2 ± 1.4
NOVI	13.5 ± 1.3	-4.0 ± 1.4	-35.6 ± 7.4
NVDO	9.2 ± 1.0	5.6 ± 1.0	3.2 ± 1.6
PENA	12.1 ± 0.9	6.5 ± 0.9	-0.9 ± 2.9
PORT	15.9 ± 1.6	6.0 ± 1.6	5.3 ± 4.9
PURI	9.4 ± 0.7	4.1 ± 0.7	2.0 ± 1.2
PZUL	9.7 ± 1.1	4.1 ± 1.1	-1.7 ± 1.9
SEBA	3.2 ± 0.8	2.2 ± 0.8	-1.5 ± 2.1
SJDL	20.0 ± 0.9	4.7 ± 0.9	-21.5 ± 3.9
TAPA	6.9 ± 0.9	2.9 ± 0.9	3.0 ± 4.1
TECO	11.2 ± 0.9	7.3 ± 0.9	-5.5 ± 1.4
TENA	21.4 ± 1.4	9.8 ± 1.4	-16.5 ± 3.7
TNCC	9.7 ± 1.7	4.6 ± 1.7	-1.6 ± 3.0
TNCM	13.3 ± 1.5	7.9 ± 1.5	-5.2 ± 2.5
TNCT	14.2 ± 2.5	6.5 ± 2.5	-1.7 ± 4.4
TNLC	10.1 ± 1.7	6.3 ± 1.7	-0.2 ± 3.0
TNMR	12.3 ± 1.5	6.7 ± 1.5	-6.1 ± 2.5
TNMZ	14.5 ± 1.8	9.8 ± 1.8	-6.3 ± 3.1
TNTM	17.6 ± 2.2	10.1 ± 2.2	-1.1 ± 4.0
TNZA	-1.6 ± 2.2	-2.2 ± 2.2	—
TOMA	27.1 ± 5.9	9.6 ± 6.3	5.0 ± 36.5
UAGU	2.1 ± 1.0	2.8 ± 1.0	—
UCOL	14.6 ± 0.8	8.9 ± 0.8	-6.5 ± 2.7
UGEO	4.1 ± 0.7	1.4 ± 0.7	-0.9 ± 1.1
UMON	3.9 ± 2.0	1.2 ± 2.0	1.3 ± 17.9
VALL	5.6 ± 3.1	-7.5 ± 3.1	-0.4 ± 5.9
VICT	10.9 ± 0.9	1.6 ± 0.9	-12.9 ± 3.7

† See footnote in Table S1.10.

Table S12: Misfit F (Eq. 1.3) and weighted root mean square error wrms (Eq. 1.4) for all models with viscoelastic relaxation corrections.

Maxwell time τ_m	F	wrms (campaign sites) mm
2.5 years	13.6	5.8
4 years	13.1	5.4
8 years	13.8	5.3
15 years	14.4	5.4
25 years	14.6	5.7
40 years	14.9	5.6
no correction	14.7	6.1

S3 SUPPLEMENTARY FIGURES

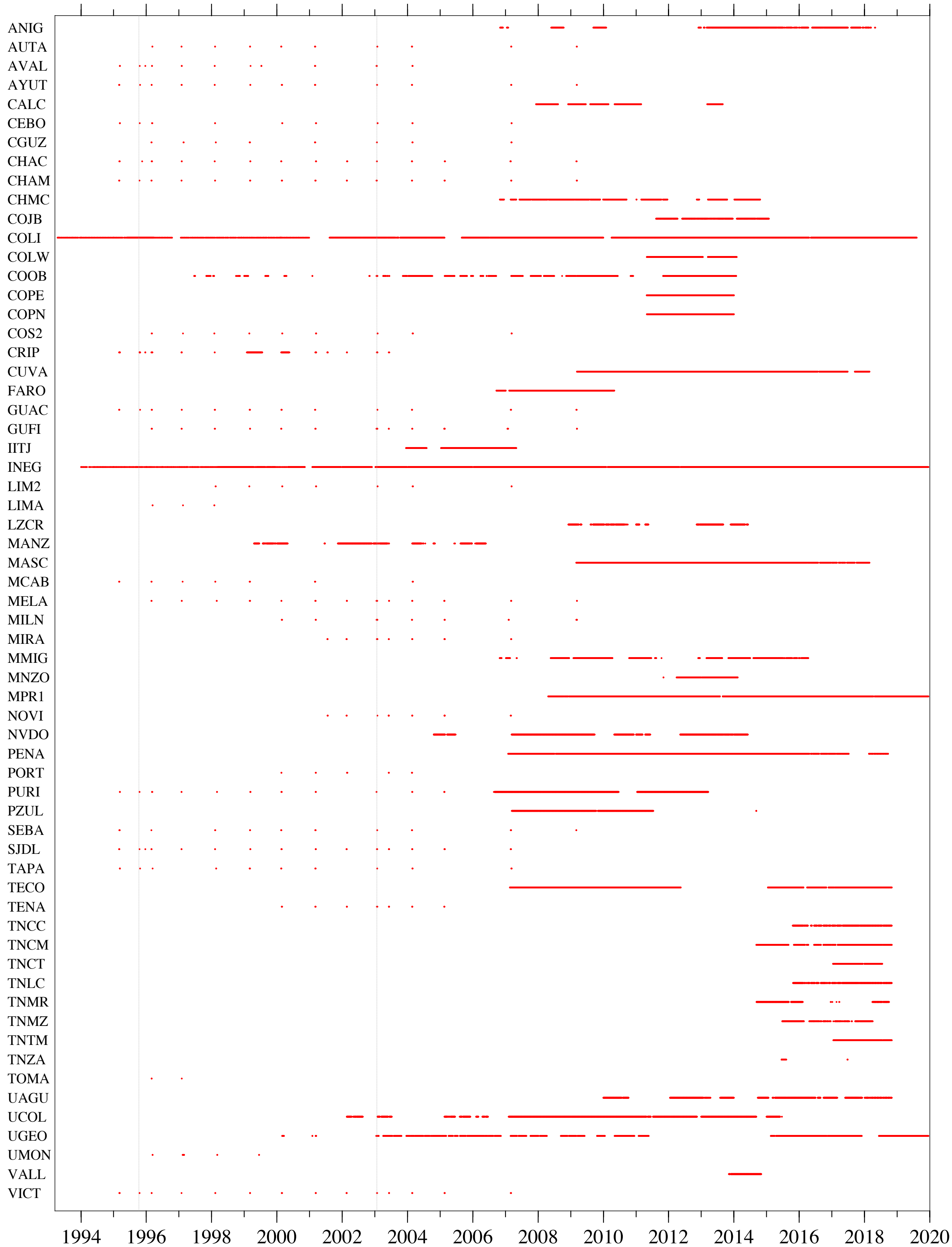

Figure S1. Time coverage of the GPS sites. Vertical lines indicate earthquake dates.

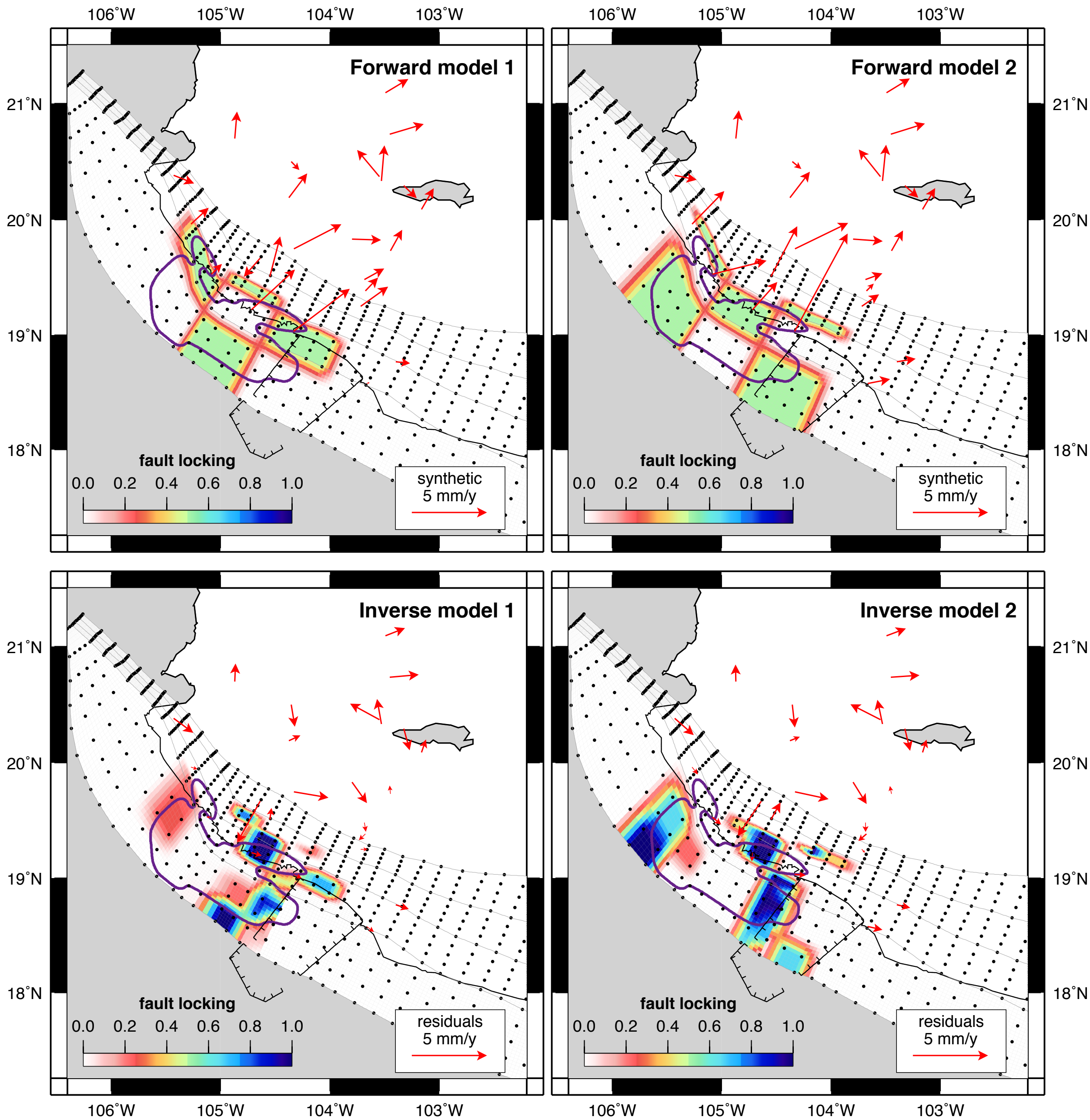

Figure S2. Checkerboard tests for the Jalisco Colima subduction zone. Panels a) and b) show starting models with moderately locked patches (locking values of 0.5) and their predicted (synthetic) horizontal GPS velocities. Panels c) and d) show locking solutions recovered from inversions of the synthetic GPS velocities with 1−σ noise added (σ = 1 mm for the north and east components, and σ = 2 mm for the vertical component) and the residuals of the horizontal site velocities from the best fitting solutions. Purple line delimits the 1995 coseismic rupture area as shown in Fig 20 of the main document.

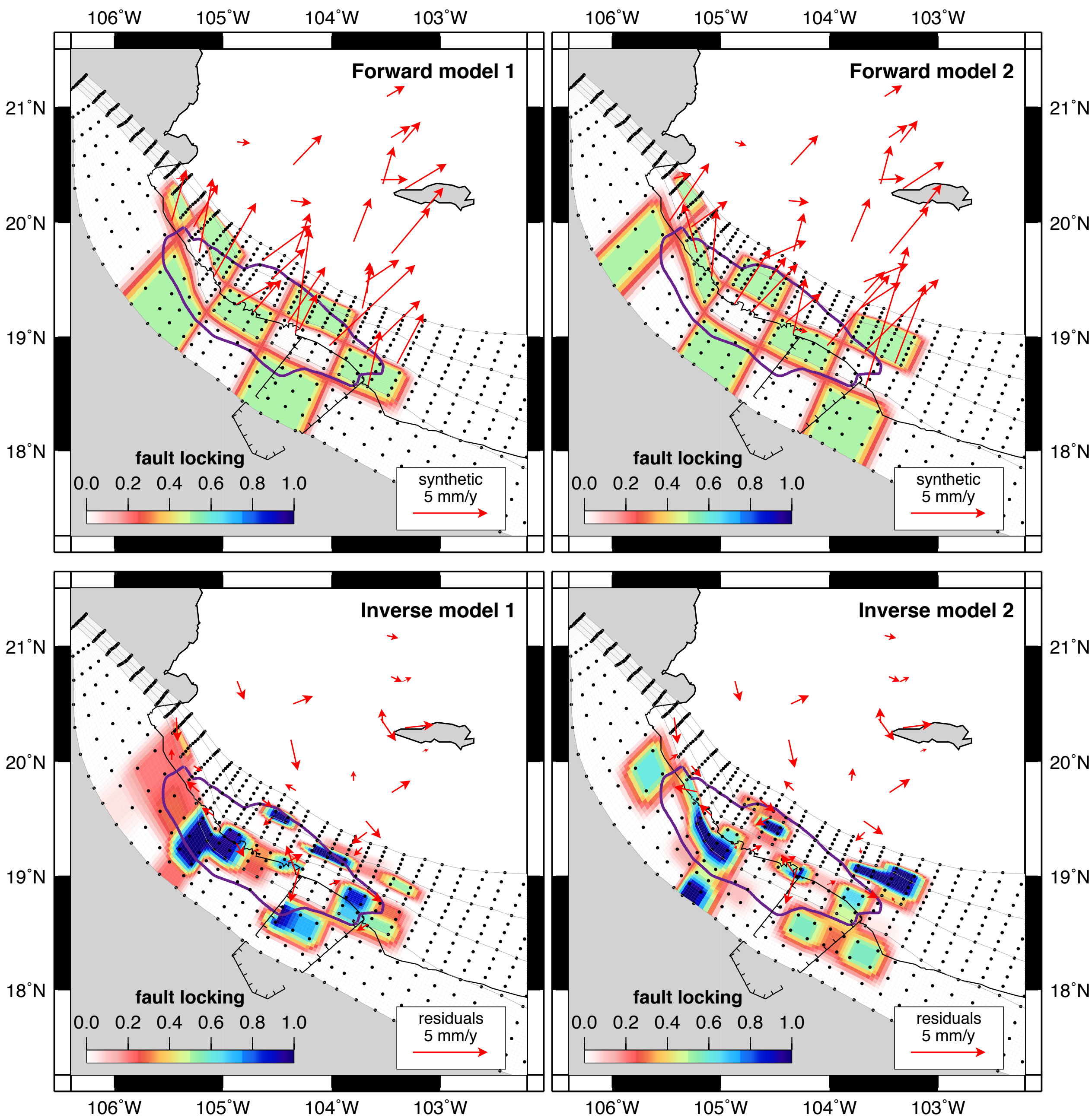

Figure S3. Checkerboard tests for the Jalisco Colima subduction zone. Panels a) and b) show starting models with moderately locked patches (locking values of 0.5) and their predicted (synthetic) horizontal GPS velocities. Panels c) and d) show locking solutions recovered from inversions of the synthetic GPS velocities with 1−σ noise added (σ = 1 mm for the north and east components, and σ = 2 mm for the vertical component) and the residuals of the horizontal site velocities from the best fitting solutions. Purple line delimits the 1995 afterslip area as shown in Fig 20 of the main document.

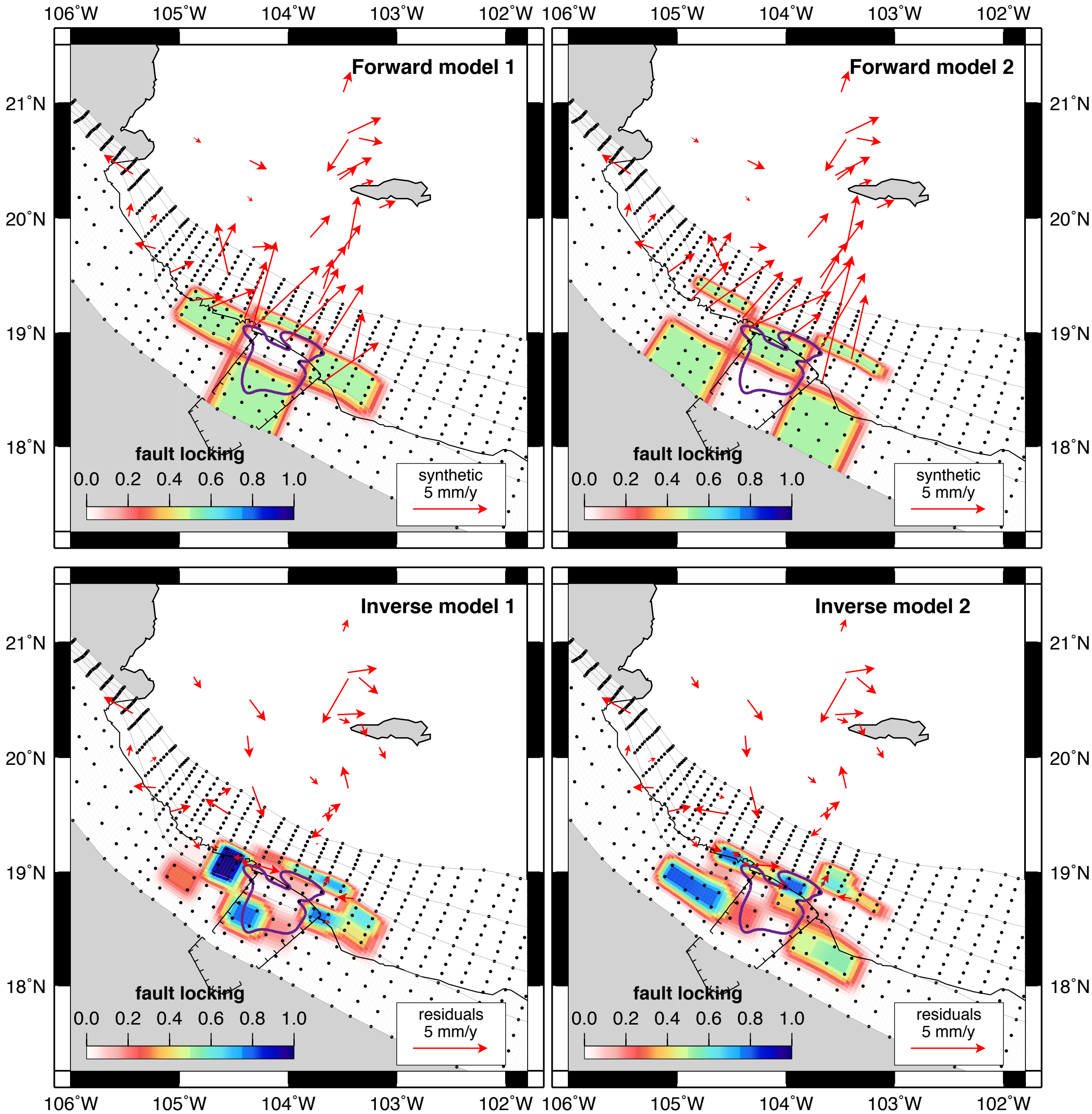

Figure S4. Checkerboard tests for the Jalisco Colima subduction zone. Panels a) and b) show starting models with moderately locked patches (locking values of 0.5) and their predicted (synthetic) horizontal GPS velocities. Panels c) and d) show locking solutions recovered from inversions of the synthetic GPS velocities with 1−σ noise added (σ = 1 mm for the north and east components, and σ = 2 mm for the vertical component) and the residuals of the horizontal site velocities from the best fitting solutions. Purple line delimits the 2003 coseismic rupture area as shown in Fig 20 of the main document.

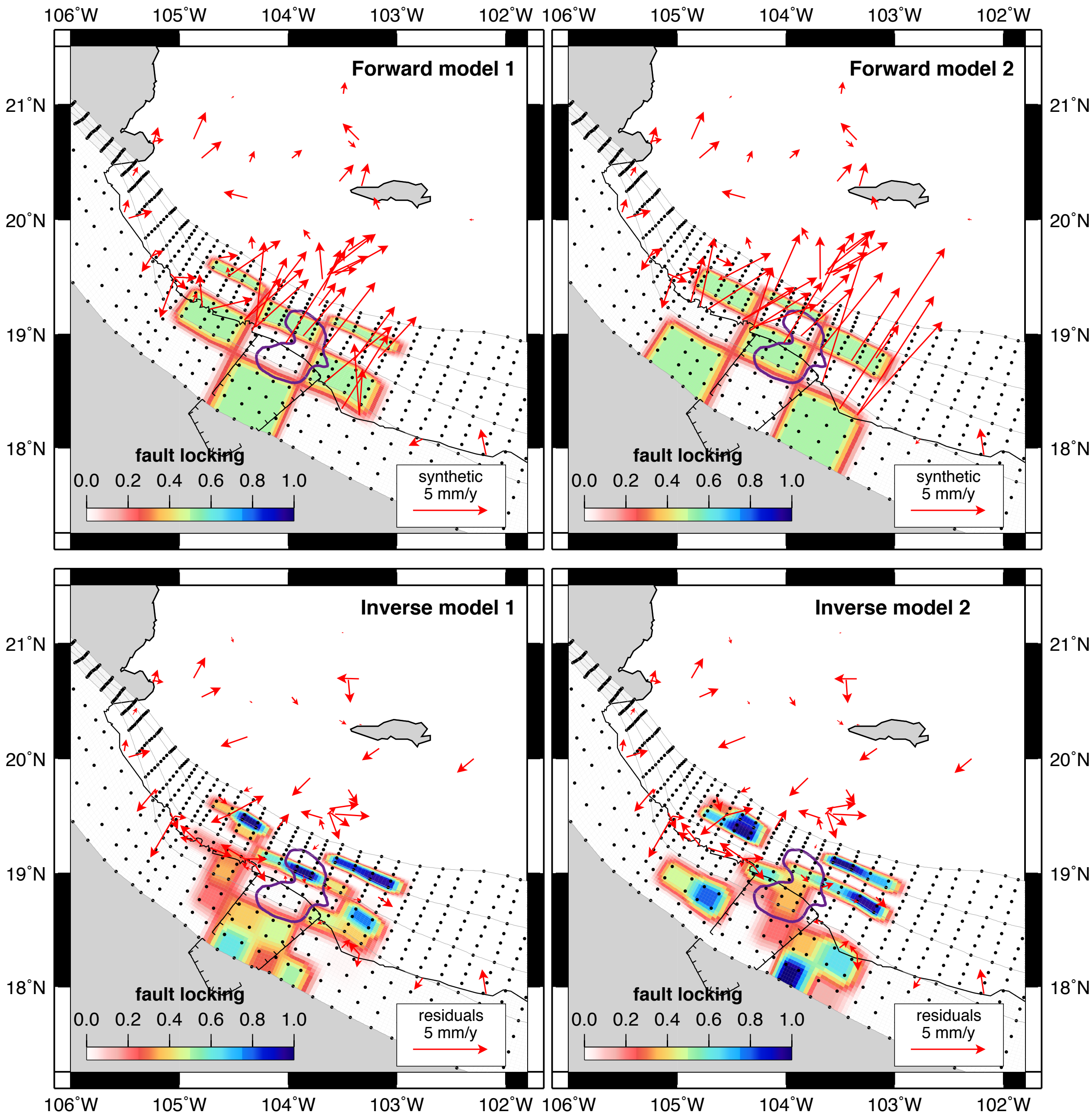

Figure S5. Checkerboard tests for the Jalisco Colima subduction zone. Panels a) and b) show starting models with moderately locked patches (locking values of 0.5) and their predicted (synthetic) horizontal GPS velocities. Panels c) and d) show locking solutions recovered from inversions of the synthetic GPS velocities with 1−σ noise added (σ = 1 mm for the north and east components, and σ = 2 mm for the vertical component) and the residuals of the horizontal site velocities from the best fitting solutions. Purple line delimits the 2003 afterslip area as shown in Fig 20 of the main document.

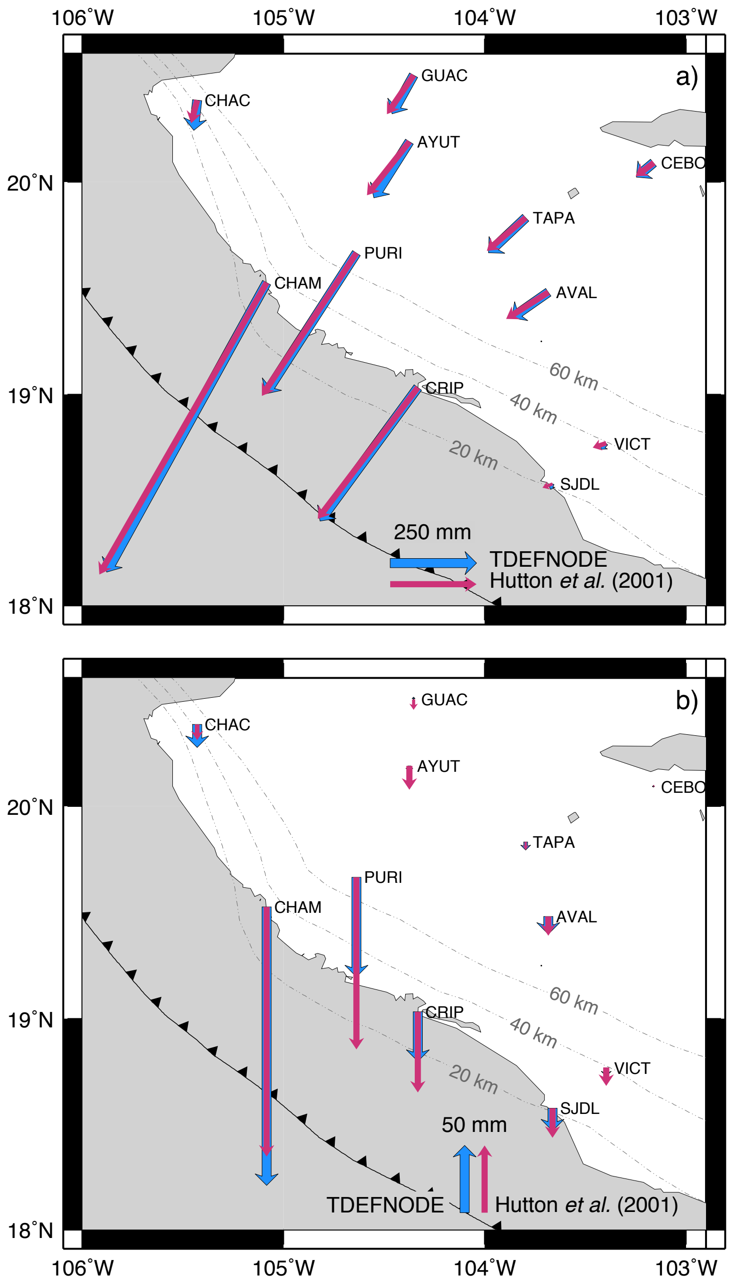

Figure S6. Coseismic GPS site displacements from the 1995 Jalisco–Colima earthquake, predicted by our preferred slip solution (blue arrows) and by the model from Hutton *et al*. (2001) (magenta arrows).

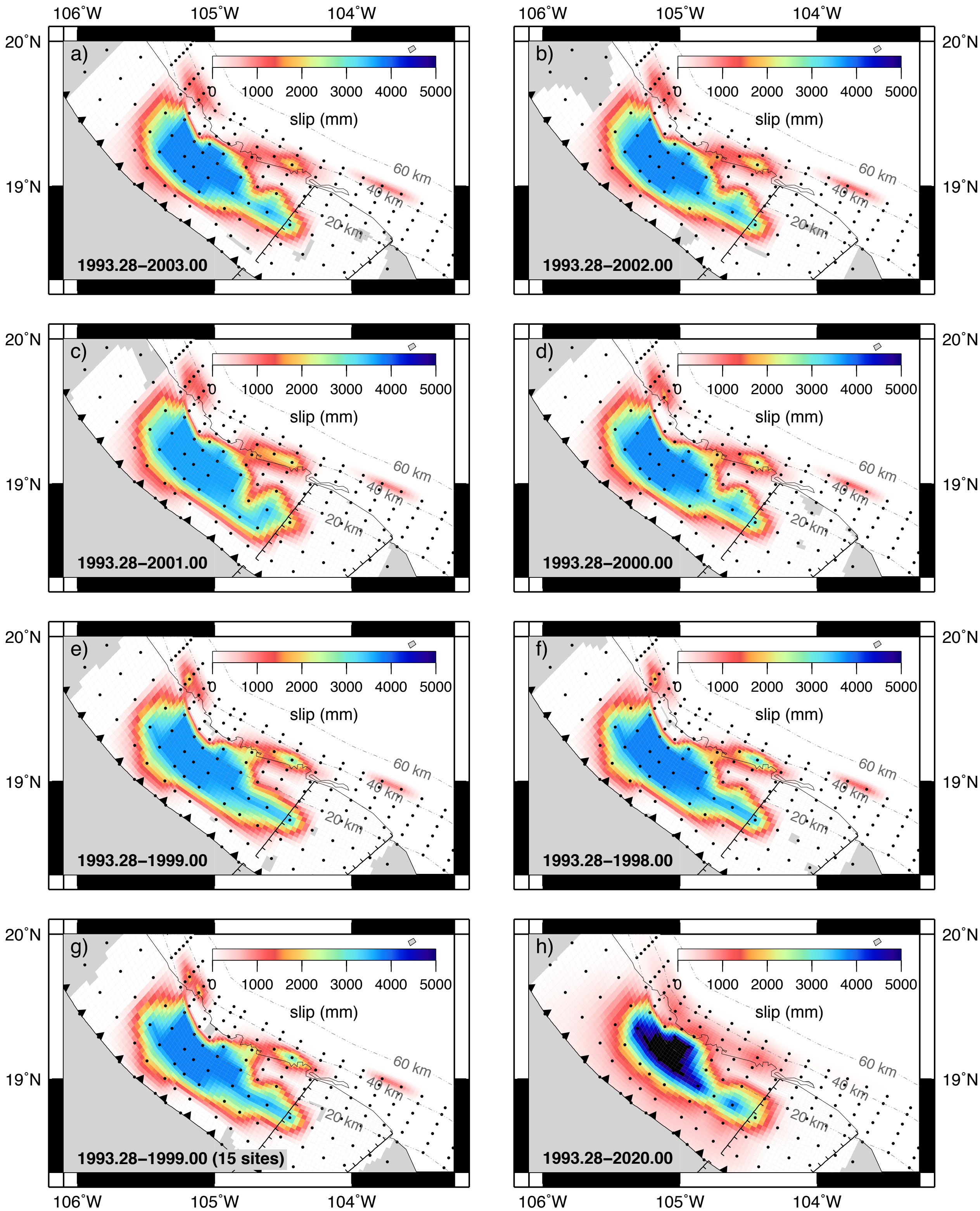

Figure S7. TDEFNODE slip solutions for the 1995 Colima–Jalisco earthquake using observations from the interval indicated on each panel. "15 sites" refers to the use of the sites active during the earthquake exclusively. Dashed lines show the slab contours every 20 km. Black dots locate the fault nodes where slip is estimated.

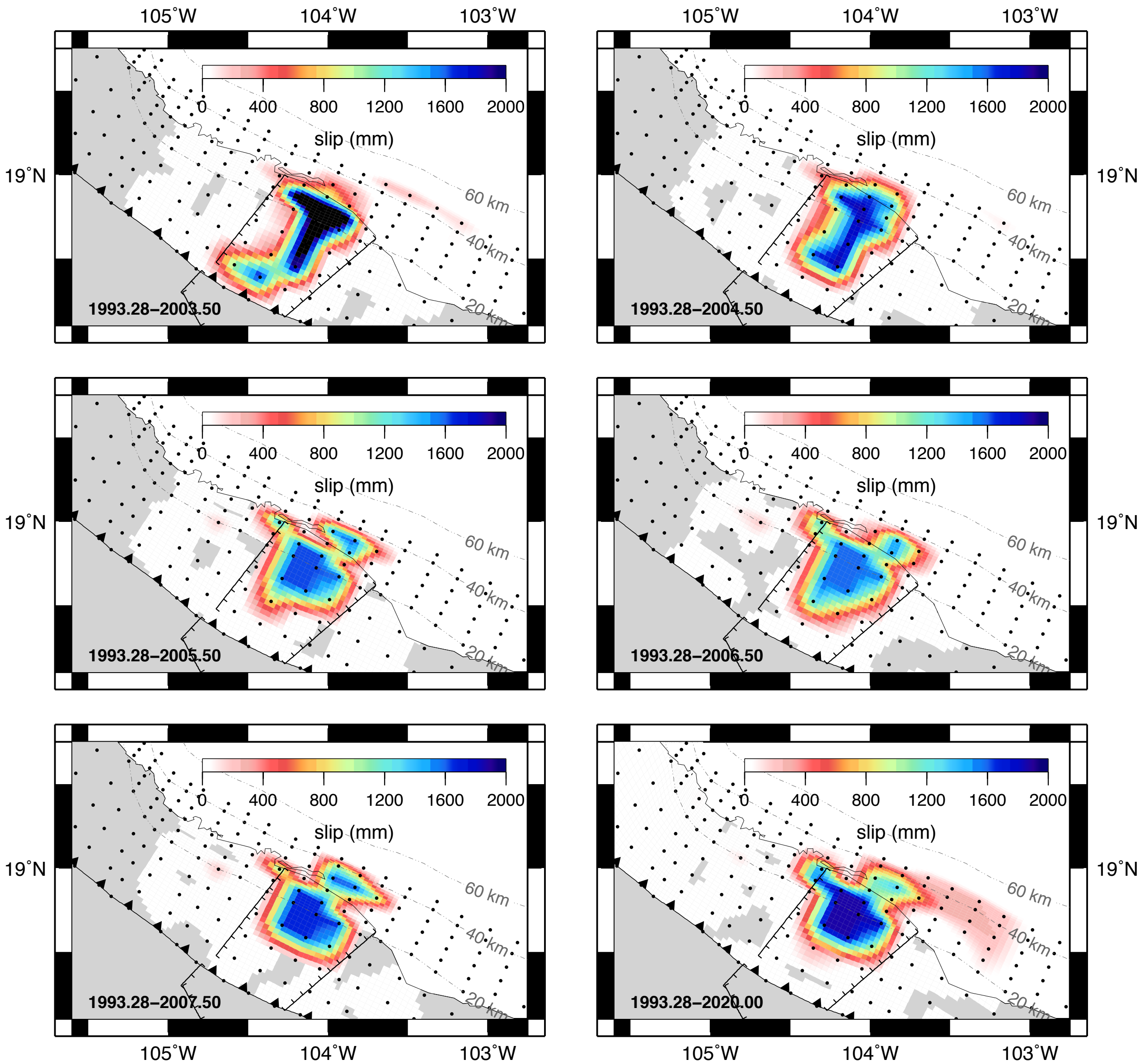

Figure S8. TDEFNODE geodetic slip solutions for the 2003 Colima–Jalisco earthquake using time series corrected for the viscoelastic effects of the 1995 Tecoman earthquake with τ_m = 15 years for the mantle. The interval used for the inversion is shown on each panel. Bottom right panel (1993.28–2020.00) corresponds to a model with no viscoelastic corrections. Dashed lines show the slab contours every 20 km. Black dots locate the fault nodes where slip is estimated.

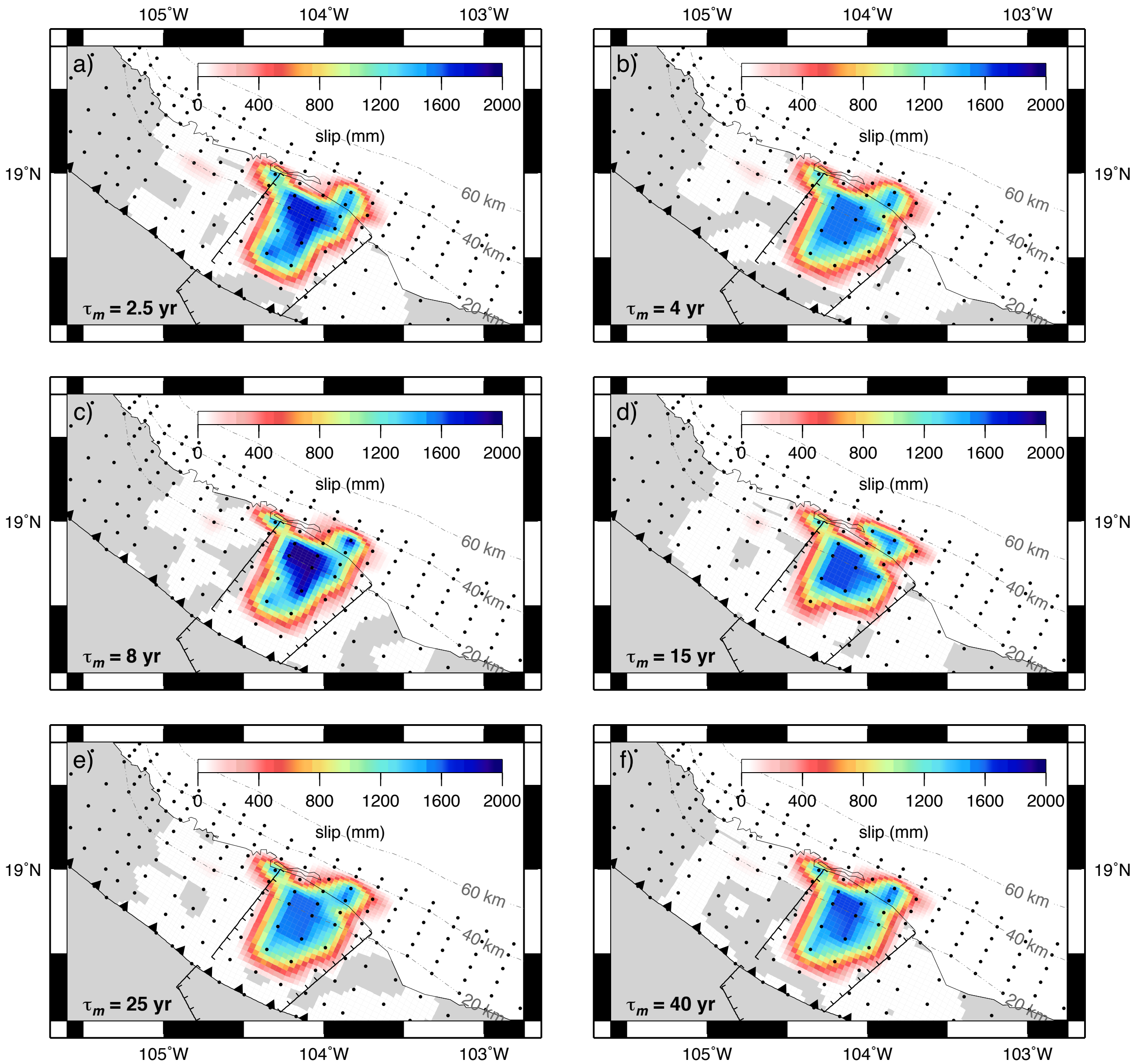

Figure S9. TDEFNODE slip solutions for the 2003 Tecoman earthquake using time series corrected for the viscoelastic effects of the 1995 Colima–Jalisco earthquake. The Maxwell time τ_m for the mantle corresponding to the correction is indicated on each panel. The interval used for the inversion was 1993.28–2005.50. Dashed lines show the slab contours every 20 km. Black dots locate the fault nodes where slip is estimated.

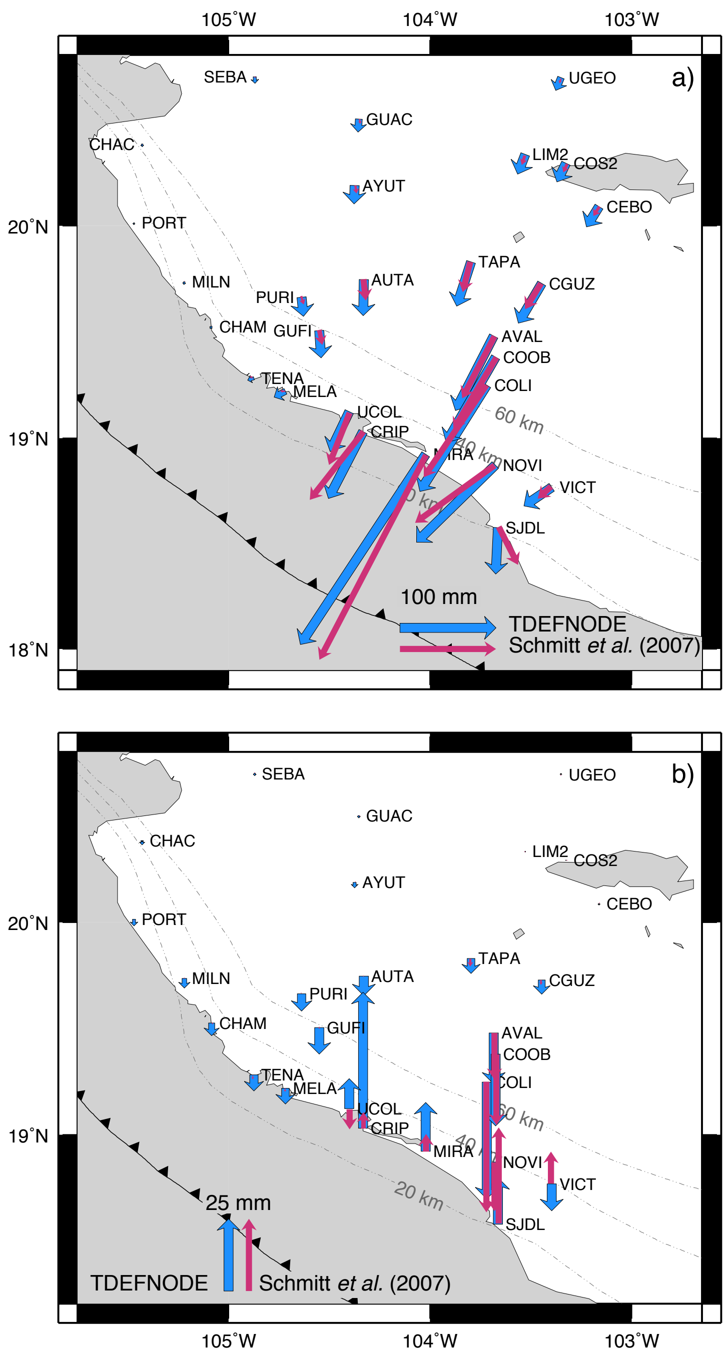

Figure S10. Coseismic GPS site displacements from the 2003 Tecomán earthquake, predicted by Schmitt *et al*. (2007) (magenta arrows) and by our preferred slip solution for the model corresponding to the correction for the viscoelastic effects of a mantle with $\tau_m = 15$ years (blue arrows).

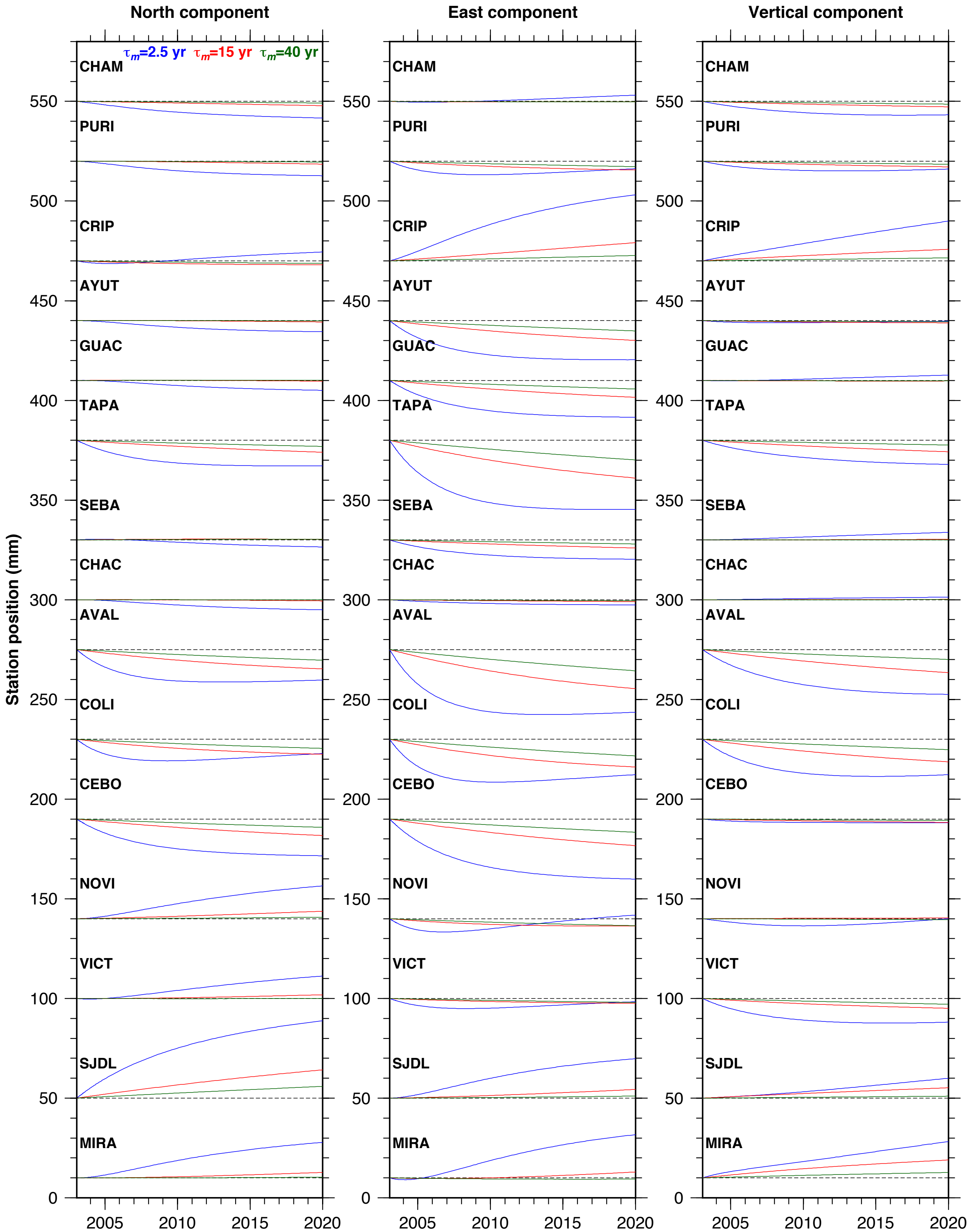

Figure S11. Modeled viscoelastic deformation for the 2003 Tecomán earthquake at selected GPS sites, for mantle rheologies corresponding to Maxwell times of 2.5 (blue), 15 (red), and 40 years (green).

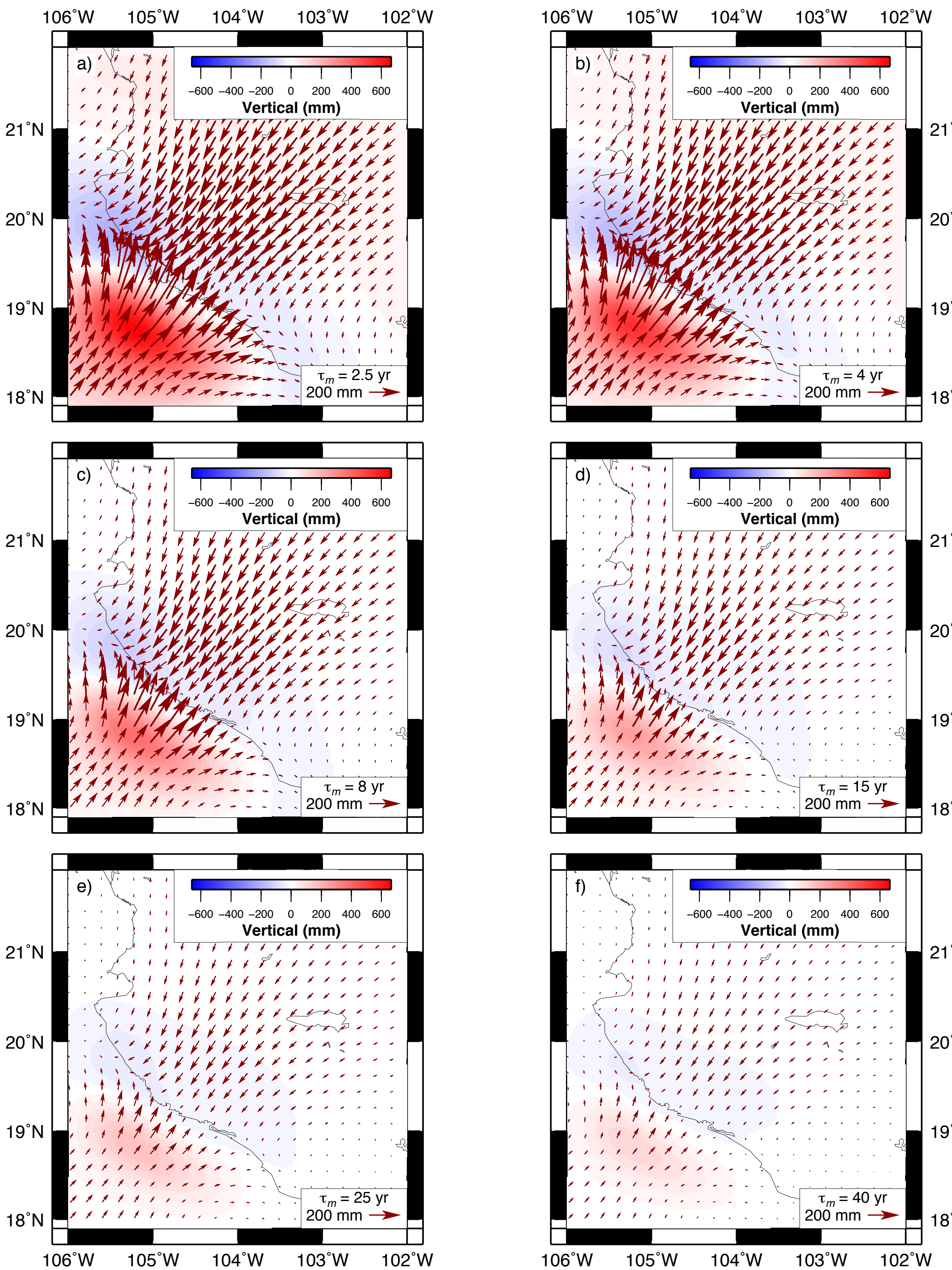

Figure S12. Cumulative viscoelastic displacements for the ~25–year–long period 1995.77 to 2020.27 triggered by the 1995 Colima–Jalisco and the 2003 Tecomán earthquakes, as predicted with RELAX software using our preferred coseismic slip solutions. The displacements shown in each panel were determined using the mantle Maxwell time given in the lower right corner of each panel. Arrows show the horizontal displacements and colors indicate the vertical displacements.

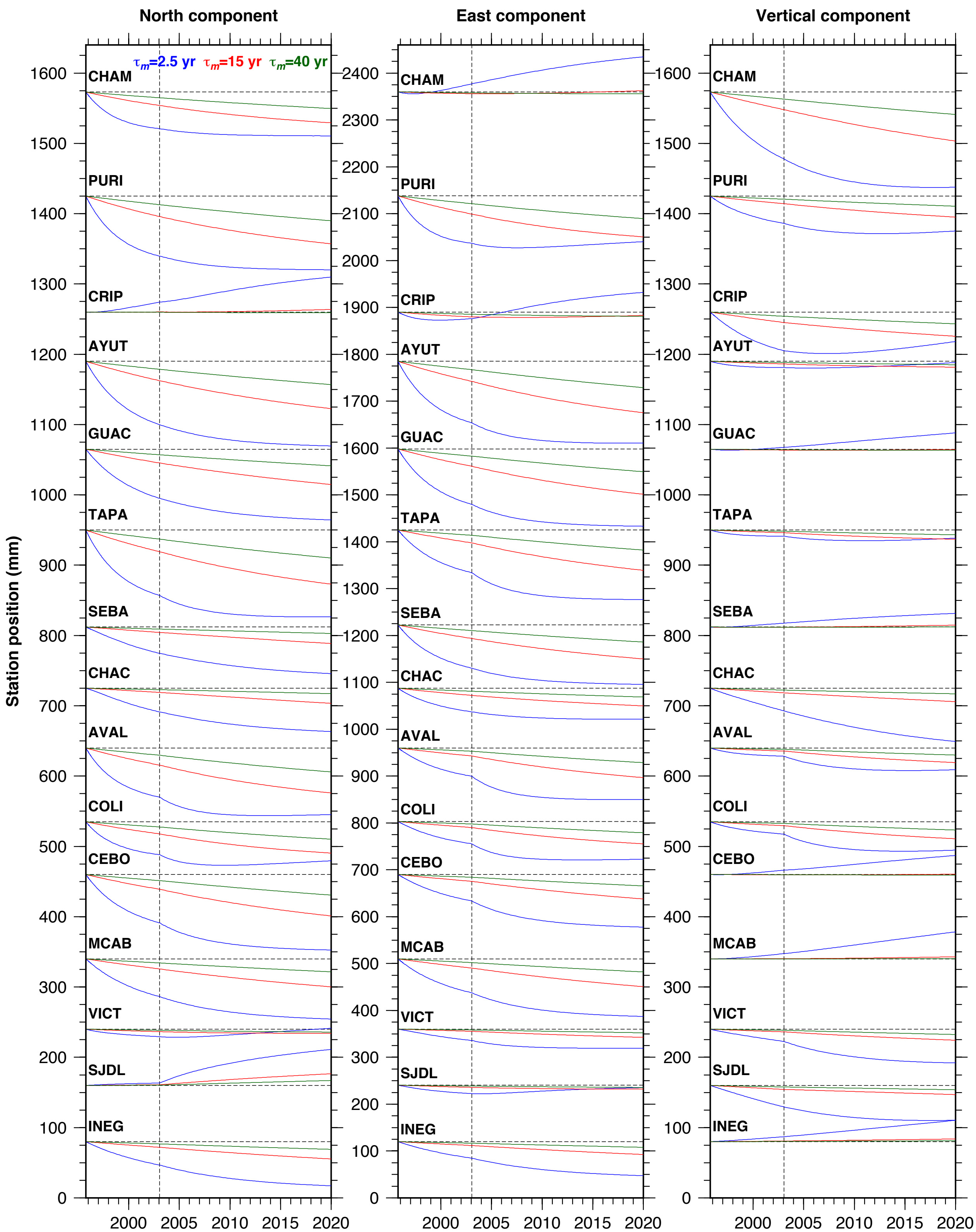

Figure S13. Modeled viscoelastic deformation for the 1995 Colima–Jalisco and the 2003 Tecomán earthquakes at selected GPS sites, for mantle rheologies corresponding to Maxwell times of 2.5 (blue), 15 (red), and 40 years (green). The dashed vertical lines mark the time of the 2003 Tecomán earthquake.

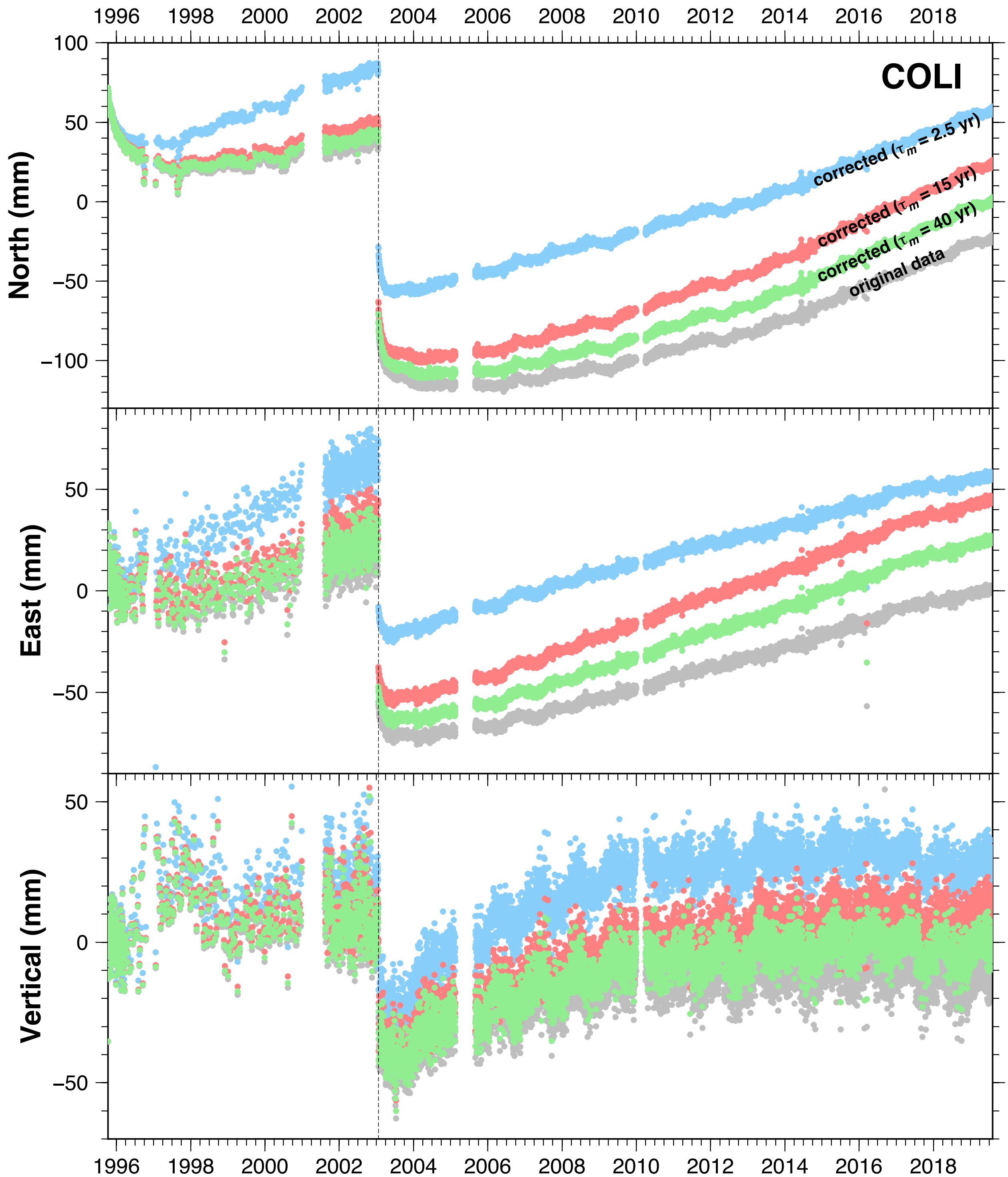

Figure S14. Daily north, east and vertical displacements for GPS station COLI, from 1993 to 2019. Gray dots correspond to the original time series. Blue, red and green dots correspond to the time series corrected for the viscoelastic deformation response from the 1995 and 2003 earthquakes, using $\tau_m = 2.5$, 15, and 40 years, respectively. The black dashed line marks the time of the 2003 Tecomán earthquake.

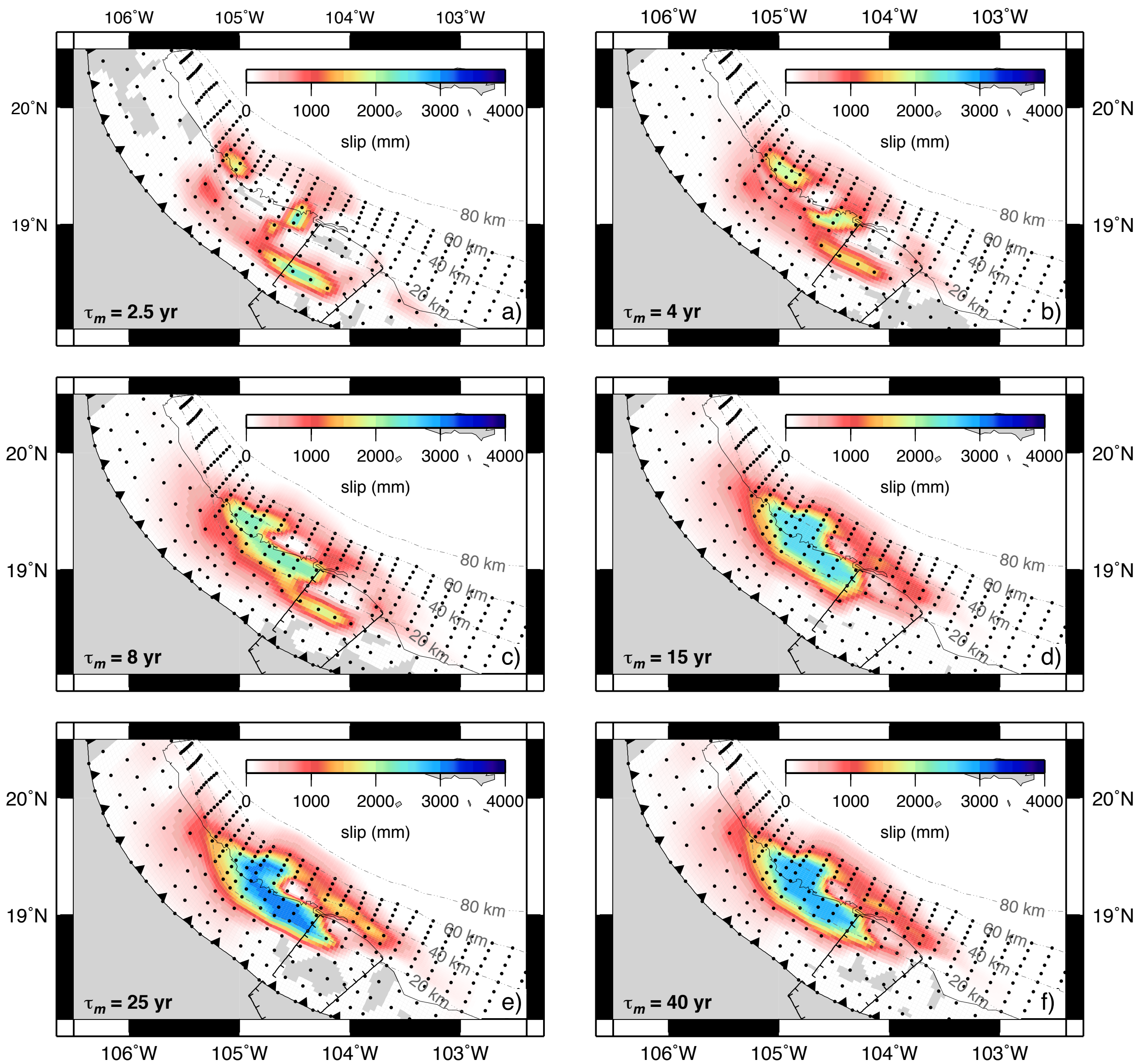

Figure S15. TDEFNODE slip solutions for the 1995 Colima–Jalisco earthquake afterslip (integrated over the 1995.77–2020.00 interval) using time series corrected for the viscoelastic effects of the 1995 Colima–Jalisco and the 2003 Tecomán earthquakes. The mantle Maxwell times τ_m used for the corrections are indicated on each panel. The interval of observations used for the inversions was 1993.28–2020.00. Dashed lines show the slab contours every 20 km. Black dots locate the fault nodes where slip is estimated.

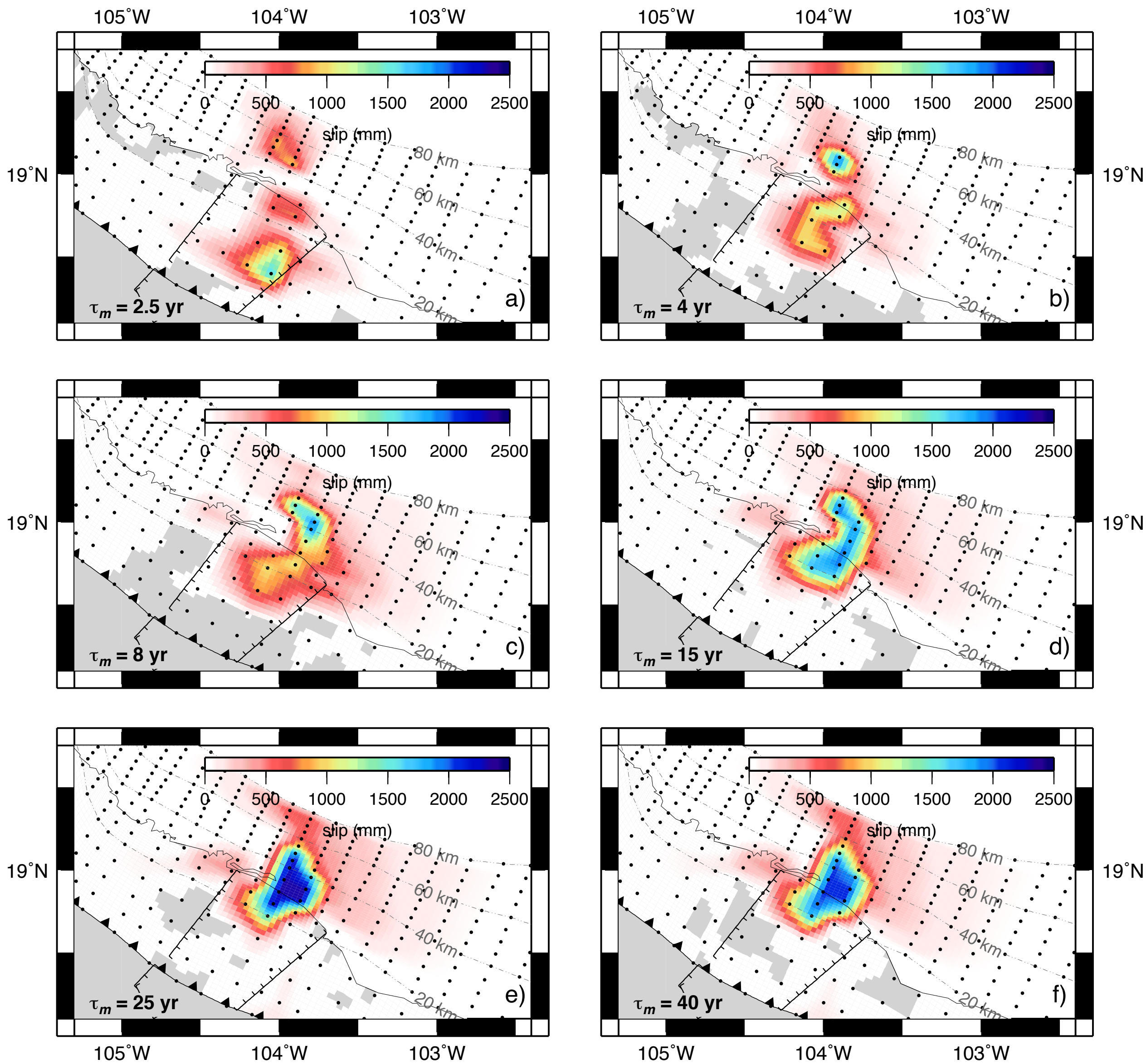

Figure S16. TDEFNODE solutions for the 2003 Tecoman earthquake afterslip (integrated over the 2003.06–2020.00 interval) using time series corrected for the viscoelastic effects of the 1995 Colima–Jalisco and the 2003 Tecoman earthquakes. The mantle Maxwell times τ_m used for the corrections are indicated on each panel. The interval of observations used for the inversions was 1993.28–2020.00. Dashed lines show the slab contours every 20 km. Black dots locate the fault nodes where slip is estimated.

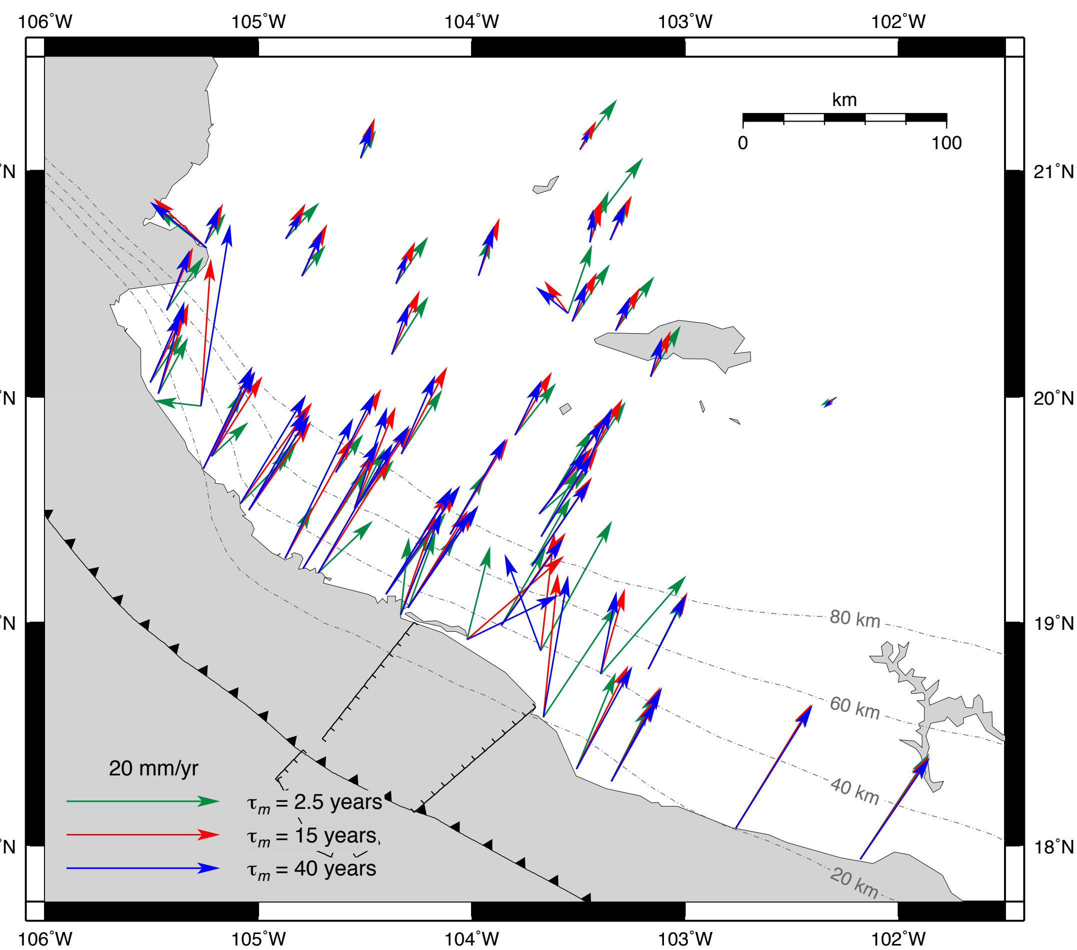

Figure S17. Best fitting horizontal site velocities relative to the North America plate, from the time–dependent inversion of GPS position time series that were corrected for viscoelastic effects using mantle Maxwel times of 2.5 (green), 15 (red), and 40 (blue) years. Uncertainties have been omitted for clarity.

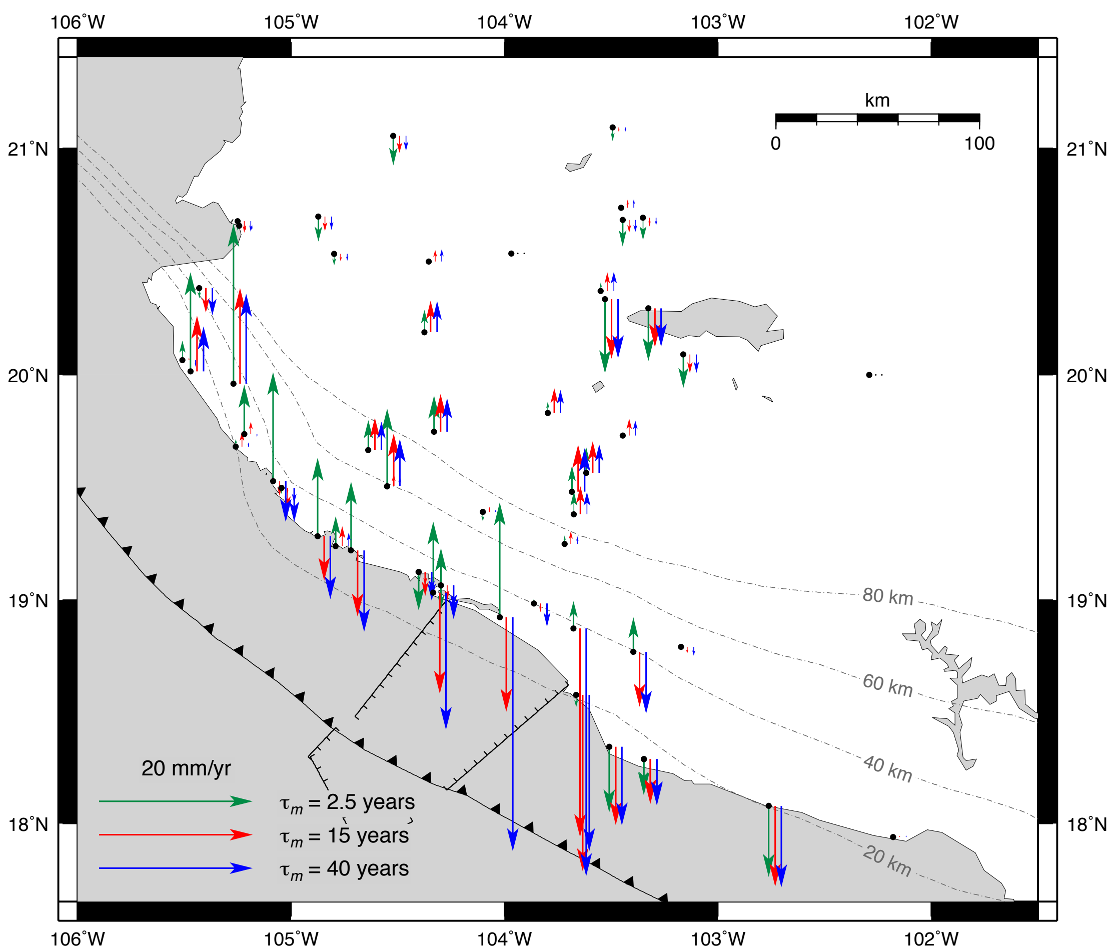

Figure S18. Best fitting vertical site velocities from the time−dependent inversion of GPS position time series that were corrected for viscoelastic effects using mantle Maxwel times of 2.5 (green), 15 (red), and 40 (blue) years. Black dots show the site locations. Superposing velocity vectors are shifted to the right to help visualization. Uncertainties have been omitted for clarity.

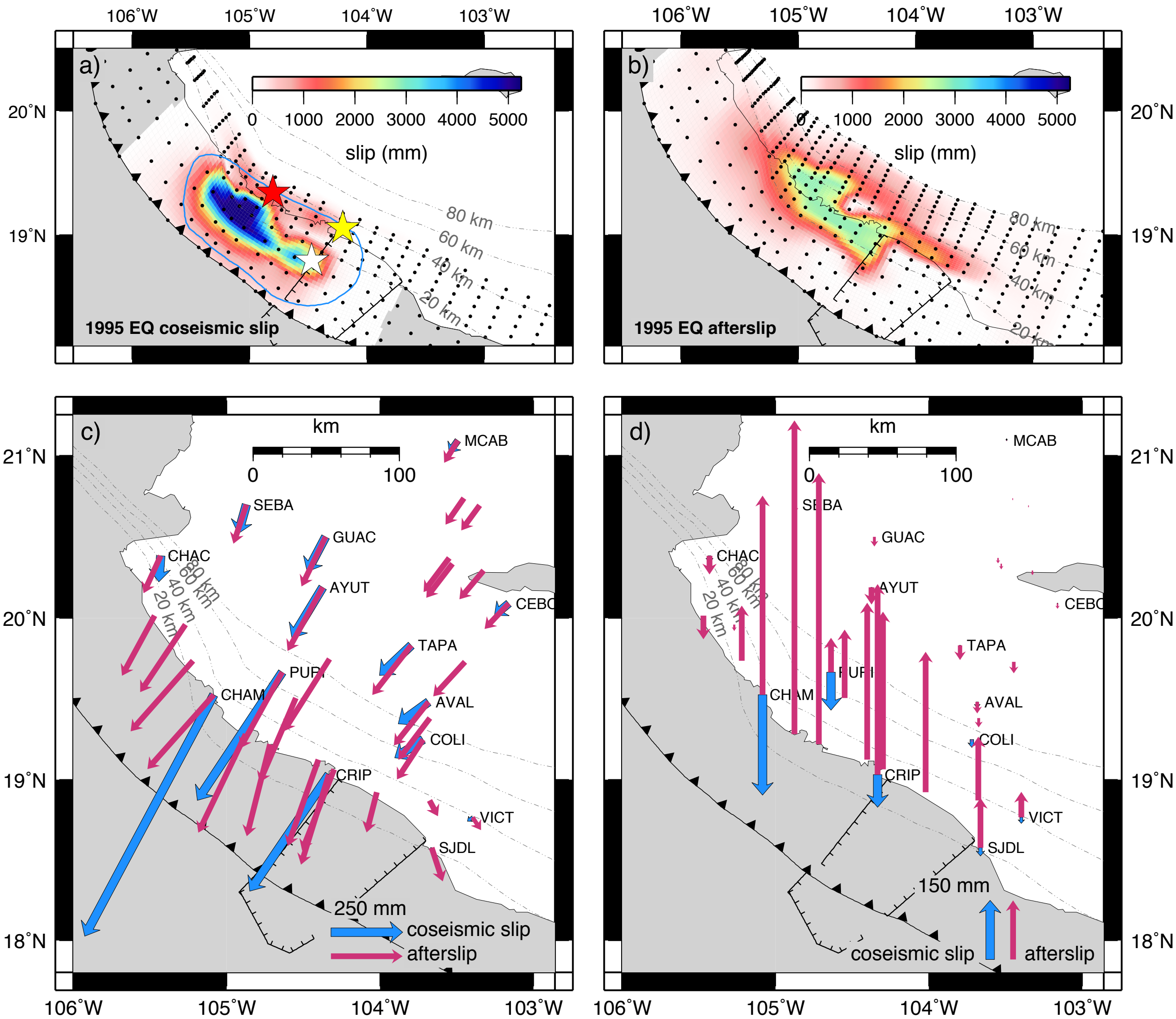

Figure S19. TDEFNODE slip solution for a) the 1995 Colima–Jalisco earthquake and b) its postseismic afterslip for a model without viscoelastic effects corrections. EQ: earthquake. Dashed lines show the slab contours every 20 km. Black dots locate the fault nodes where slip is estimated. The blue line delimits the earthquake aftershock area (Pacheco *et al*. 1997). White, yellow and red stars are the epicenters from Courboulex *et al*. (1997) and USGS, and the centroid from the gCMT catalog (Dziewonski *et al*. 1997), respectively. Panels c) and d) respectively show the horizontal and vertical site motions that are predicted by the coseismic and afterslip solutions from panels a) and b) at sites active during the earthquake for panel c) and sites active between 1995 and 2003 for panel d).

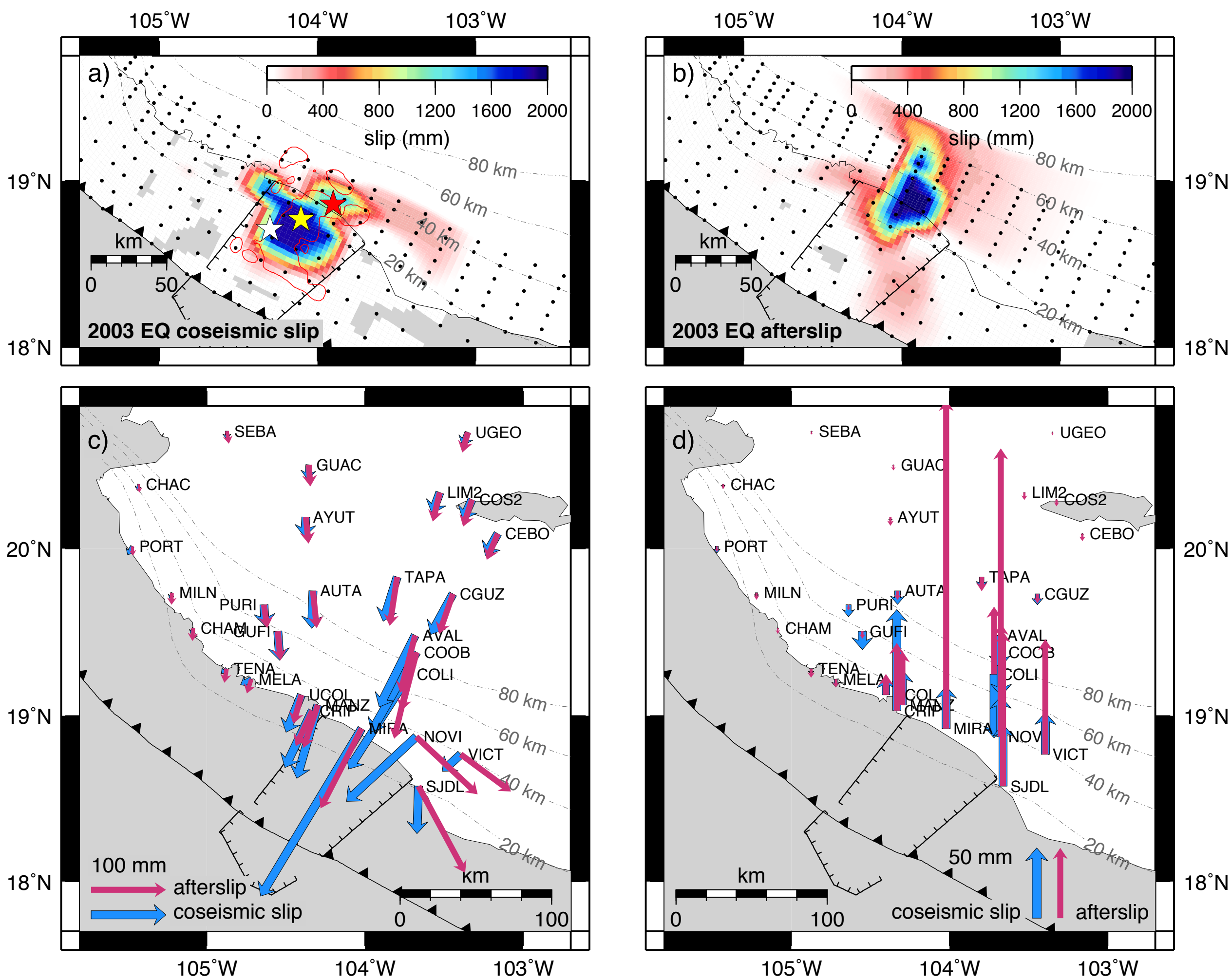

Figure S20. TDEFNODE slip solution for a) the 2003 Tecomán earthquake and b) its postseismic afterslip for a model without viscoelastic effects corrections. EQ: earthquake. Dashed lines show the slab contours every 20 km. Black dots locate the fault nodes where slip is estimated. The red line delimits the rupture area for the earthquake (Yagi *et al*. 2004). White, yellow and red stars are the epicenters from Yagi *et al*. (2004) and USGS, and the centroid from the gCMT catalog (Ekström *et al*. 2004), respectively. Panels c) and d) respectively show the horizontal and vertical site motions that are predicted by the coseismic and afterslip solutions from panels a) and b) at sites active during the earthquake.

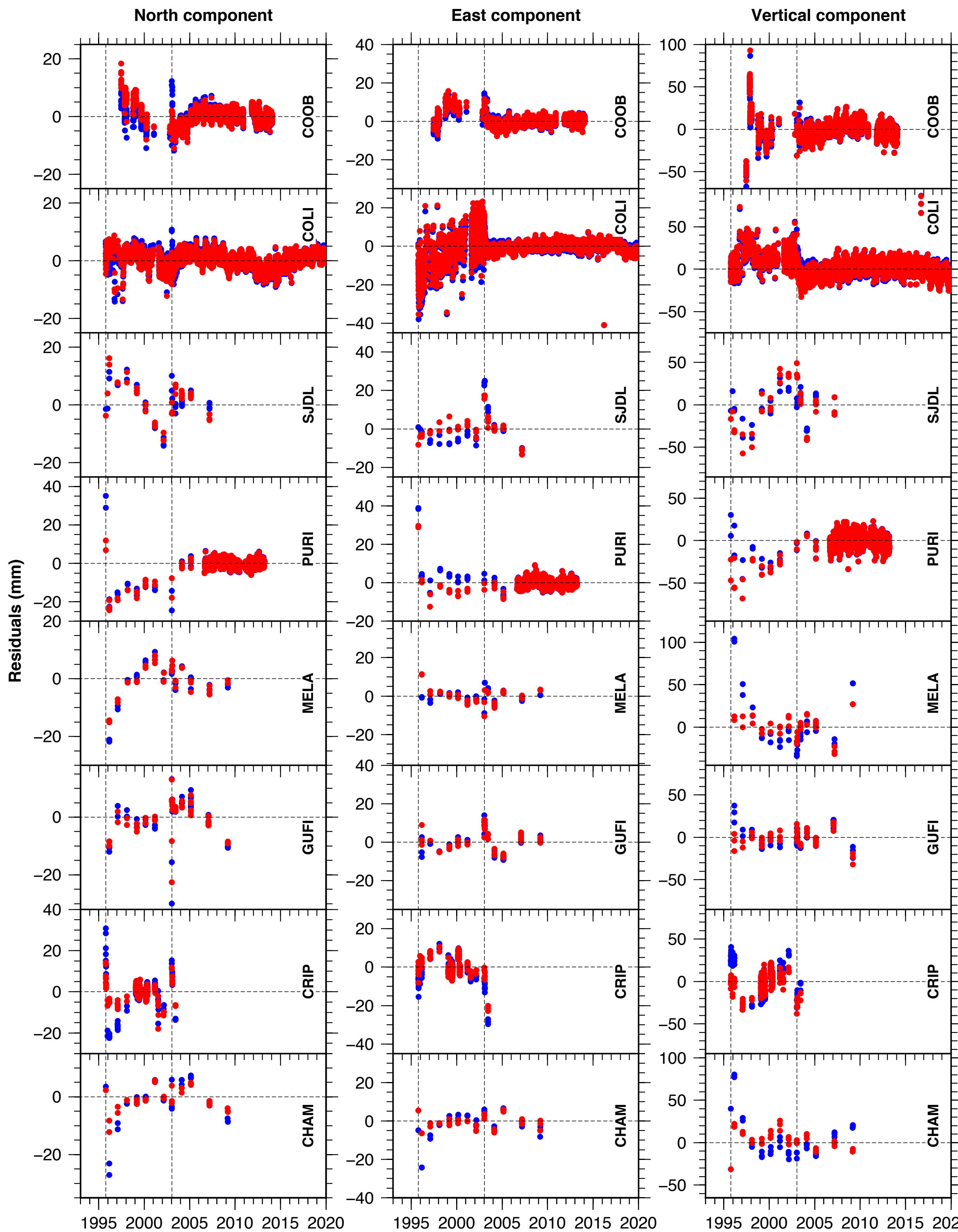

Figure S21. Residuals at selected sites from our model with viscoelastic corrections using $\tau_m = 8$ years for the mantle (red) and with no corrections for viscoelastic effects (blue). Dashed vertical lines mark the time of the 1995 and 2003 earthquakes.

S4 DESCRIPTION OF ADDITIONAL FILES

The contents of the files with our coseismic slip and afterslip solutions for the 1995 and 2003 earthquakes from our preferred model (with viscoelastic response corrections estimated with a mantle Maxwell time of 15 years) are organized as follows:

.nod files: Contain the information of the transient at the nodes. The contents of each column are:

1. Node X-index
2. Node Z-index
3. Node Longitude
4. Node Latitude
5. Node depth (km)
6. Node transient slip amplitude
7. East component* of transient slip at node (mm)
8. North component* of transient slip at node (mm)
9. Azimuth* of transient slip at node
10. Along strike distance X of node (from first node) in km
11. Across strike (horizontal) distance of node from surface node up-dip from it, in km
12. Downdip distance W of node from surface node up-dip from it, in km
13. Moment associated with this node in N m.

* Foot wall relative to hanging wall

.atr files: Contain the information of the transient at the fault discretized in fault patches (the segments joining two neighboring nodes are subdivided into five sub-segments, so that each quadrilateral generated by adjacent nodes along-strike and down-dip is subdivided into 25 constant-slip patches). The files include fault attributes and quadrilaterals that can be used to make color plots of slip distributions. Only patches with slip larger than 0.5 mm are listed. Every header line starts with > -Z for columns 1 and 2. The rest of the columns are:

3. Fault number
4. Slip amplitude (mm)
5. Strike-slip component
6. Dip-slip component
7. Fault opening component
8. East component of slip
9. North component of slip
10. Rake angle on sub-segment
11. Sub-segment centroid longitude
12. Sub-segment centroid latitude
13. Sub-segment centroid depth (km)
14. Transient number
15. Node X-index
16. Node Z-index
17. Sub-segment X-index
18. Sub-segment Z-index
19. Date of transient at patch
20. Slip at the center of the patch
21. Area of patch (km^2)

The header line is followed by the four coordinates of the trapezoid that defines the fault patch:

Lon1 Lat1 Depth1

Lon2 Lat2 Depth2

Lon3 Lat3 Depth3

Lon4 Lat4 Depth4

To plot a colored slip distribution on a map you can use the gmt script line:

```
awk '{ if ($1 ==">") print $1,$2,$4; else print $1,$2 }' filename.atr | psxy
-Cpalette.cpt -R...
```

.txt files: The columns of the files with the interseismic site velocities resulting from the models with different Maxwell times for the viscoelastic corrections, and those from the model with no correction are:

1. Site
2. North component of velocity (mm/yr)
3. 1-sigma uncertainty of the North component of velocity (mm/yr)
4. East component of velocity (mm/yr)
5. 1-sigma uncertainty of the East component of velocity (mm/yr)
6. Vertical component of velocity (mm/yr)
7. 1-sigma uncertainty of the vertical component of velocity (mm/yr)